

https://dspace.org/

The form factors of South African trees: is it possible to classify them easily using field measurements and photographs?

Muzite, Tapiwa

2017

http://hdl.handle.net/10539/23582

Muzite, Tapiwa (2017) The form factors of South African trees: is it possible to classify them easily using field measurements and photographs?, University of the Witwatersrand, Johannesburg, <http://hdl.handle.net/10539/23582>

Downloaded from a DSpace repository. https://dspace.org/

UNIVERSITY OF THE WITWATERSRAND



The form factors of South African trees: Is it possible to classify them easily using field measurements and photographs?

A research report submitted to the Faculty of Sciences, University of the Witwatersrand, Johannesburg in partial fulfilment of the requirements for the degree of Masters of Science in Environmental Sciences

(Coursework and Research Report)

2017

by

Tapiwa Muzite

Student number 1270788

Supervisor: Professor R.J Scholes

Declaration

I declare that this dissertation is my own, unaided work except where acknowledged. It is being submitted for the degree of Master of Science in Environmental Sciences, in the University of the Witwatersrand, Johannesburg. It has not been submitted before for any degree or examination in any other university.

Tapiwa Muzite

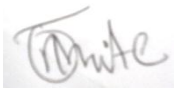

On the 26th day of May 2017

Abstract

Modern tree biomass allometry makes use of "form factor", which is the ratio of the true volume to the apparent volume. However, there is no database of form factors of South African trees, hence this study was undertaken to assess the possibility of assigning form factors to trees in a quick and easy way, either by visual assessment of an image of the tree or by simple field measurements. Stem diameter, taper and node length data for 112 trees was collected using both *in situ* and in-lab measurements from photos taken of the same trees in the field. The data were used to model tree volume using the fractal properties of branching architecture. The estimated tree volume was then used along with basal diameter and tree height to calculate the form factor.

Results showed that measurements taken off images underestimated stem diameter and node length by 4% and 5% respectively, but the fractal allometry relationships developed using either the manual in-field or image analysis approach were not statistically different. This proves that dry season photography is sufficiently accurate for establishing relationships needed to construct a fractal model of tree volume. The image analysis approach requires a clear unobstructed view of the sample tree. This requirement made the approach less effective as when trees were in close proximity and when branches overlapped. The time taken using the photographic approach was twice the amount taken for the manual in-field.

Form factor varied between species, but the variation was not statistically significant ($p=0.579$). The mean form factor per species ranged from 0.43 to 0.69. Form factors were negatively correlated with wood density (-0.177), basal diameter (-0.547) and height (-0.649). Due to the unavailability of an independent tree biomass dataset, it was impossible to validate the allometric equations based on estimated form factors and wood density. The inclusion of form factor was shown to improve the accuracy of biomass estimation by 11%.

Principal component analysis showed that form factors can be assigned using tree height and the form quotient.

Dedication

I dedicate this project to my family especially my parents for their psychological and financial support.

Acknowledgements

Special thanks go to my academic supervisor Professor R.J. Scholes for his guidance and constructive criticism during the course of this project, as well as providing financial support for data collection. I would also like to thank the staff at Wits Rural Facility (WRF), namely Professor W. Twine for his guidance and logistical support during my data collection, Mr Thabo Moyo and Mr Frank Nyathi who were my field assistants, Mr Christopher Rankin and the WRF drivers who occasionally helped in transporting us around the facility. I am also very much grateful to the staff at the South African Environmental Observation Network (Ndlovu Node, Phalaborwa), namely the Research Manager Dr Tony Swemmer, who allowed me to work at their offices to collect data on the study species that were not found at WRF, Miss Thembi Marshall who helped in arranging for our accommodation at the SAEON research guest house.

I am also indebted to Mr Alec Naidoo, the Botanist at the Pretoria Botanical Gardens who helped in facilitating data collection at the gardens for *Portulacaria afra*, Mrs Kathleeen Smart who provided witness disk samples for *P.afra* and Mr Thibedi Moshoeu for his help with the map showing the study areas. Thanks also go to administrative staff of the School of Animal, Plant and Environmental Sciences for their valuable assistance during the course of my study and the technical staff, namely Mr Bruce Patterson and Mr Bongi Hlalukane who organized for me to use the Phytotron Laboratory of the school.

Above all I would like to thank the Lord God Almighty for His grace, throughout the whole project.

Table of Contents

Declaration i

Abstract ii

Dedication iii

Acknowledgements iv

List of Figures viii

List of Tables ix

List of acronyms and symbols xi

Chapter 1 1

Background 1

Aim of the Research 3

Objectives 3

Literature review 4

Biomass assessment 4

Use of allometric equations in biomass estimation 5

Fractal allometry 6

Traditional forms of allometric equations and the new universal form 8

Form factor 11

Relationship between form factor and other tree dimension attributes 13

Assigning tree form factor by visually assessing a tree image 13

Photo-based measurement of tree dimensions 14

Sites and study species 16

Sampling and the photography of the trees 18

Procedure for data collection 19

Calculation of tree biomass using the Fractal allometry programme 21

Statistical analyses 23

Model fitting 23

Comparisons of new allometry with existing empirical allometry 23
Trend analysis for form factors 26
Chapter 3: Results 27
Comparisons of regression formulae derived from *in situ* and image measurements 27
Time required to collect allometric data 29
Model fitting 31
Researcher's vs Colgan *et al*. (2013) form factors 34
Comparisons between equations 34
Effect of form factor on model precision 40
Form factor and its correlation with the other predictor variables 41
Pattern analysis of form factors 42
Chapter 4: Discussion 45
Comparisons of regression formulae derived from in situ and image measurements 45
Model fitting and the comparisons between the new and existing empirical allometry 46
Form factor and its relationship with other tree attributes 47
Estimation of form factors from easily observable tree traits 48
Chapter 5: Conclusion 50
References 51
Appendix 1: The fractal allometry programme 56
`Fractal allometry programme (Courier font 10).` 56
Appendix 2: An example of an input file for the FractalGu programme, showing the input parameters for *T.sericea* 63
Appendix 3.1: Summary of regression formulae for the relationship between branch ratio (unit less) and stem diameter (cm). 64
Appendix 3.2: Summary of regression formulae for the relationship between branch taper and stem diameter (cm). 66
Appendix 3.3: Summary of regression formulae for the relationship between internode length (cm) and stem diameter (cm). 68

Appendix 3.4: Summary of regression formulae for the relationship between bark thickness (mm) and the logarithm of stem diameter (cm). 70

Appendix 4.1: Comparisons of the log-regression coefficients of the new allometry (Researcher's) and the standard form of the empirical allometry. 71

Appendix 4.2: Comparisons of the factor (b) and power (a) of the new allometry equation (Researcher's) and the existing empirical allometry. 72

Appendix 5: The 95% confidence intervals for the slope (β_1) and intercept (β_0) used to compare the new allometry (Researcher) to the existing empirical allometries. 73

List of Figures

Figure 1.1: A tree as a fractal object made up of parts (branches) similar to the whole tree. ...7

Figure 2.1: The locations of the two study sites where data collection was done.…. ...…….17

Figure 2.2: Measurements points for the collection of data for the fractal allometry.…….21

Figure 3.1: *In situ* versus image measurements of stem diameter (a) and node length (b). 27

Figure 3.2: Researcher's species-specific equations relating the logarithm of biomass (kg) to the logarithm of the compund variable ($F\rho D^2H$). 33

Figure 3.3: Comparisons of the standard form ($M= bD^a$) of the new allometry and empirical allometry……..….36

Figure 3.4: The 95% confidence intervals of the slope of the standard equation form {ln (M) = (β_0 + $\beta_1$ln($F\rho D^2H$)} for the species specific and species neutral new allometry, empirical allometry and the Colgan *et al*. (2013) species neutral allometry 38

Figure 3.5: The 95% confidence intervals of the intercept of the standard equation form {ln (M)=β_0 +$\beta_0$ln($F\rho D^2H$)} for the species specific and species neutral new allometry, empirical allometry and the Colgan et al. (2013) species neutral allometry. 39

Figure 3.6: Species specific equations relating the logarithm of biomass (kg) as estimated from the Colgan *et al*., (2013) equation for that species, to the logarithm of the compound variable (ρD^2H).. 40

Figure 3.7: Ordination plot showing the distribution of form factors for individual trees of each species, with each colour representing a different species. The axis F1 and F2 are mainly related to tree height and form quotient, respectively.....44

List of Tables

Table 1.1: Approximate theoretical values of β under different scenarios. 10

Table 2.1: Ample locations and sizes 16

Table 2.2: Colgan *et al*. (2013) species-specific equations and the species neutral equation (ALL) of the form $\ln(M)=\beta_0+\beta_1\ln(D^2H)$; relating stem diameter D (cm) and height H (m) to biomass (kg)…….24

Table 2.3: Nickless *et al*. (2011) species-specific equations of the form $\ln(M)=\beta_0+\beta_1\ln(D)$ relating stem diameter D (cm) to biomass (kg)……24

Table 2.4: Species-specific equations by Tietema (1993) and Shackleton (1998) expressed in the original form $\ln(M)=b+a\ln(D^2H)$; relating stem diameter D (cm) and height H (m) to biomass (kg). The original form was also converted to the standard form $M=bD^a$; relating stem diameter (cm) to biomass (kg); where "b" is the factor and "a" is the power…….24

Table 3.1: ANOVA results for the relationship between branch ratio and stem diameter (cm). 29

Table 3.2: ANOVA results for the relationship between branch taper and stem diameter (cm). 30

Table 3.3: ANOVA results for the relationship between node length (cm) and stem diameter (cm). 30

Table 3.4: ANOVA results for the relationship between bark thickness (mm) and stem diameter (cm). 31

Table 3.5: Species-specific biomass allometric equations, relating form factor (m^{-3}/ m^{-3}), field wood density (kg/ m^{-3}), basal stem diameter (m), and height (m) to biomass (kg)…….. 32

Table 3.6: Comparisons between form factors derived by the researcher and those by Colgan *et al*. (2013)……..34

Table 3.7: Comparisons of the slope and intercept of the equations derived from fractal allometry to that of empirical allometries by the different authors……..34

Table 3:8: ANOVA results showing how the form factors varied by basal stem diameter and species. 41

Table 3.9: Correlation amongst the predictor variables**,** with significance at 1% and 5% level, representing by * and ** respectively, where r is the Pearson correlation coefficient .....…….42

Table 3.10: The amount of information (eigenvalues) and variation (variability %) in form factor accounted for by each principal component. 43

Table 3.11: Squared cosine values reflecting the representation quality of each variable along principal components F1 to F8. 43

List of acronyms and symbols

F – form factor

ρ - wood density

D – basal stem diameter

H – canopy height

Mg – megagrams

kg – kilograms

g – grams

m^{-3} - per cubic metre

m – metres

cm – centimetres

mm – millimetres

dbh - diameter at breast height

r^2 - coefficient of determination

SE – standard error

ln – natural logarithm

exp - exponential

π – pi - ~ 3.142

μ – mean

σ - standard deviation

df – degrees of freedom

F – Fishers test

Sig – significance

spp – species

r – Pearson’s correlation coefficient

TS – *Terminalia sericea*

SB – *Sclerocarya birrea*

CA – *Combretum apiculatum*

DC – *Dichrostachys cinerea*

LS – *Lannea schweinfurthii*

CM – *Colophospermum mopane*

CI – *Combretum imberbe*

PA – *Portulacaria afra*

IPCC – Intergovernmental Panel on Climate Change

Chapter 1

Background

The United Nations Framework Convention on Climate Change recognises the capability of forests, woodlands and savannas to sequester and store carbon (Samalca, 2007), but this capability has not been fully evaluated (Da Silva *et al*., 2015). This has made the assessment of tree biomass a highly pertinent contemporary issue in relation to global change (Bombelli *et al*., 2009; Da Silva *et al*., 2015). Field measurements are the most used approach in biomass assessment, as they are more accurate than remote sensing and GIS-based approaches (Lu, 2006). The traditional approach for field measurements has been to cut down trees, measure their stem diameters and weigh components (for example twigs and branches) so as to calculate biomass; but such an approach is time consuming, destructive and expensive (Netshiluvhi and Scholes, 2001, Nickless *et al*., 2011). The solution is to predict biomass from an easily measured tree dimension parameter such as diameter, using the principle of allometry (Netshiluvhi and Scholes, 2001, Nickless *et al*., 2011).

Allometry is the relationship between changes in the size of one part of an organism to changes in its overall size (Gayon, 2000). In forestry, the basic principle of allometry is evident in that, proportions between biomass and diameter follow the same rules for trees growing under the same conditions (Picard *et al*., 2012). This means that a difficult to measure variable for example tree biomass can be predicted from an easier to measure dimension for example diameter, using an allometric equation, thereby providing a potentially simple and quick method of estimating biomass (Netshiluvhi and Scholes, 2001). Allometric equations are simple mathematical forms of equations that express the relationship between a dependent variable for example biomass and an independent variable for example diameter (Netshiluvhi and Scholes, 2001). A major problem with this approach is that such arbitrary relationships vary from species to species and from site to site (Nickless *et al*., 2011), and this results in an inconsistent choice of allometric equations. The massive costs associated with the establishment of allometric equations have also contributed to obstacles which hinder the estimation of the overall biomass of tropical forests and woodland comprised of many different species (Kamatou, 2003). Tree species occurring in tropical forests and woodlands are mostly of low commercial value and therefore have never had empirical allometries developed (Kamatou, 2003).

Recent approaches to estimating biomass have attempted to address the problem of the arbitrary and inconsistent choice of allometric relationships by proposing universal forms of equations based on geometric logic and adjusted for species using a form factor (Návar, 2010). Mass rather than volume is derived from the universal equations by using wood density, conventionally given the symbol "ρ and units Mg m^{-3} (Návar, 2010). The new allometric equation is in the form

$$M = \beta_0 + \beta_1(F\rho D^2 H) \qquad \text{[equation 1]}$$

where M is biomass (expressed as dry mass in Mg); β_0 and β_1 are model coefficients, F is form factor, ρ is wood density (in Mg m^{-3}); D is stem diameter (in m) and H is total height (in m) of the tree from the ground to the top of the canopy, excluding stray branches which might extend above the canopy.

From the new allometry, the stem diameter and height can be easily measured and there are databases, for example Van Wyk (1974) and www.worldagroforestry.org on the wood density of many African species. However, there is no database for the form factors of different tree species, making it a challenge to use the new allometry. At present, it is either necessary to assume a standard form factor for all trees in a broad forest type such as tropical rainforest or tropical dry forest, which then reduces the accuracy of the biomass or volume estimate; or to measure the form factor for each species, which is nearly as much work as to estimate species-specific empirical allometries. The challenge is to devise a sufficiently accurate way of estimating form factors for South African species without the trouble and expense of cutting a large number of trees.

One approach is to model the volume of a tree without weighing it, the approach being based on the fact that a tree is made up of many similar parts of itself (Sala, 2013). A model of the tree volume based on fractal properties of its branching architecture provides a potentially quicker and non-destructive method of estimating tree volume, which can then be used along with basal diameter and canopy height to calculate form factor (Kamatou, 2003).

Aim of the Research

To determine if the form factors of South African trees can be easily assigned, thereby improving the accuracy of biomass estimation.

Objectives

(1) To estimate the form factors of a sample of representative species using fractal allometry.

Key questions and hypotheses:

a) Are dry-season photographs an efficient and sufficiently accurate way to collect the data needed to construct a fractal model for tree volume?
b) How does an allometry equation built from physical principles (involving form factor, wood density, height and diameter at the base) compare with existing empirical allometries?

   H1: physically-based allometries have equal or better precision and accuracy than empirical allometries.
c) Does the inclusion of a species-specific form factor improve species-specific models?

   H2: Inclusion of a species form factor increases the precision of biomass estimation relative to equations not including a form factor.
d) Is the form factor related to wood density or any other tree attribute?

   H3: Form factor is independent of wood density or any other tree attribute.

(2) To assess if form factor can be assigned to trees without destructive harvesting or time consuming field measurements.

e) Is it possible to allocate the form factors with sufficient accuracy from a visual inspection of the tree or a few simple measurements taken from the photographs?

   H4: Form factor can be assigned to trees without destructive harvesting or time consuming measurements.

Literature review

Biomass assessment

Biomass is defined as the living and dead organic matter (Bombelli *et al*., 2009), and consists of the above ground components (foliage, reproductive structure, branches including twigs, main stem and stump) and the below ground component which is made up of coarse and fine roots (Samalca, 2007). Forest biomass serves as both a source and sink of carbon, thus the amount of carbon stored in vegetation globally is greater than that stored in the atmosphere (Bombelli *et al*., 2009). This means that any changes in vegetation cover as a result of forest degradation or deforestation affects the amount of carbon in the atmosphere (Bombelli *et al*., 2009). Land use changes to a large extent involving changes in biomass, account for about a fifth of the anthropogenic forcing of the global climate (Le Quéré *et al*., 2016), thereby making biomass assessment a very important issue climate change modelling (Bombelli *et al*., 2009; Da Silva *et al*., 2015). In addition to the important role that it plays in the evaluation of stocks and fluxes of carbon (Návar, 2010), biomass assessment also enables the monitoring of resource availability and use through the quantification of fuelwood or timber at a given time (Samalca, 2007). Since the energy content of wood is strongly related to its mass, estimating the biomass allows the quantification of the primary energy which can be obtained from trees as a substitute for fossil fuels (Návar, 2010).

Many studies have focused on the assessment of above-ground forest biomass because it accounts for the majority of the biomass in a forest (Samalca, 2007). This is less true in drier woodlands and savannas, where a large part of the biomass may be underground. However the technical difficulties of measuring below-ground biomass mean that above-ground biomass is almost inevitably used as a proxy for total biomass, after applying an "expansion factor" to account for underground biomass (Konôpka *et al*., 2011).

Breidenbach *et al*. (2014) state that, "the uncertainty associated with biomass assessment is important in the further use of the assessment results in policymaking and international reporting. Nations that have signed the United Nations Framework Convention on Climate Change are obliged to report estimates and uncertainties for their biomass assessment (IPCC, 2000). The uncertainty also shows the quality of the biomass assessment thereby revealing its weaknesses, and this serves as the basis for identifying areas for possible improvement in such assessments (Breidenbach *et al*., 2014).

The first source of uncertainty in biomass estimation is associated with sampling errors in the selection of sample plots, with the size of the error being affected by the sampling scheme, sample size, estimation procedure (Samalca, 2007). Sampling errors can be reduced by randomly selecting the sample plots in a stratified approach (Henry *et al*., 2015).

Measurement errors are the second source of the uncertainty in biomass estimation and they can occur as a result of the type of instrument used, improper use of the correct measurement instrument, recording error and the nature of the object being measured for example an irregular girth (Chave *et al*., 2005; Shettles *et al*., 2015). Measurement error has two parts, the random error which tends to zero as the sample size increases; and the systematic error for example inclusion of buttresses in the measurement of tree diameters (Brown *et al*., 1995). The systematic measurement error does not tend to zero even if the sample size is increased, and should therefore be avoided by all means possible (Samalca, 2007).

The third source of uncertainty is the model error which is as a result of variation in the residuals around model predictions (Shettles *et al*., 2015). Applying the same model to all trees also contributes to the systematic error, but this is avoided or corrected for by independent calibration and validation (Shettles *et al*., 2015). In most biomass assessment studies, it is usually only the sampling error that is accounted for and this results in the total uncertainty of biomass estimations being under-estimated by a large factor (Shettles *et al*., 2015).

Above-ground biomass has been assessed using remote sensing, GIS-based approaches and field measurements (Samalca, 2007). Though the three approaches can be jointly used to map biomass stocks across landscapes, the problem with remote sensing and the GIS-based approach is that they are not be accurate at the relevant spatial scales as compared to filed measurements (Lu, 2006). However the massive costs and destructive harvesting of sample trees associated with field measurements result in allometry being the preferred method of estimating biomass (Nickless *et al*., 2011).

Use of allometric equations in biomass estimation

Návar (2010) states that, "the development and application of allometric models is the standard methodology for above-ground biomass estimation". Allometric models can be classified as empirical, semi-empirical or theoretical, based on the methods of parameter estimation (Návar, 2010).

Empirical allometry involves the destructive harvesting of sample trees and measurement of diameter and height, followed by the cutting of the trees into the main biomass components (stem, branches and leaves) (Kamatou, 2003). The components will then be weighed so as to measure their fresh weight and then small subsamples are oven dried in the laboratory to a constant weight at 70°, to determine their initial water content (Kamatou, 2003). This value then allows the dry weight of the tree to be calculated from the field-measured wet weight (Návar, 2010)**.** The dry to fresh weight ratios are multiplied by the total fresh weight of each component so as to calculate the total dry biomass for each (Návar, 2010)**.**

Historically, allometric equations have been entirely empirical, based on the destructive sampling of individual trees (Kamatou, 2003). In the past few decades, approaches have been proposed for parameter estimation without having to fell any sample trees, an example being the use fractal properties of tree branching architecture (Návar, 2010)**.**

Fractal allometry

Sala (2013) defines a fractal as "a fragment geometric shape that can be sub-divided into parts which are similar to the whole shape in some way". A tree can be divided into segments "branches", with each branch having a similar shape to the whole tree (Sala, 2013). The underlying reason why a tree is a fractal is the conservation of the transport vessel cross-sectional area between the roots and terminal branches, coupled with the similar physical constraints under which all parts of the tree must function (MacFarlene *et al*., 2014). The fractal properties of tree branching architecture make it possible to estimate tree biomass through fractal allometry (Kamatou, 2003). Fractal allometry enables the estimation of the total stem volume (V) from a measurement of the stem diameter (D), and then the repeated application of the set of single-node branching and taper rules which govern the recurrent patterns of tree branches until some defined terminal diameter is reached (Van Noordwijk and Mulia, 2002). The measurements which define the "rules" can be made in a relatively quick and non-destructive manner as compared to empirical allometry which requires felling, drying and weighing of a large number of trees (Kamatou, 2003; Picard *et al*., 2012).

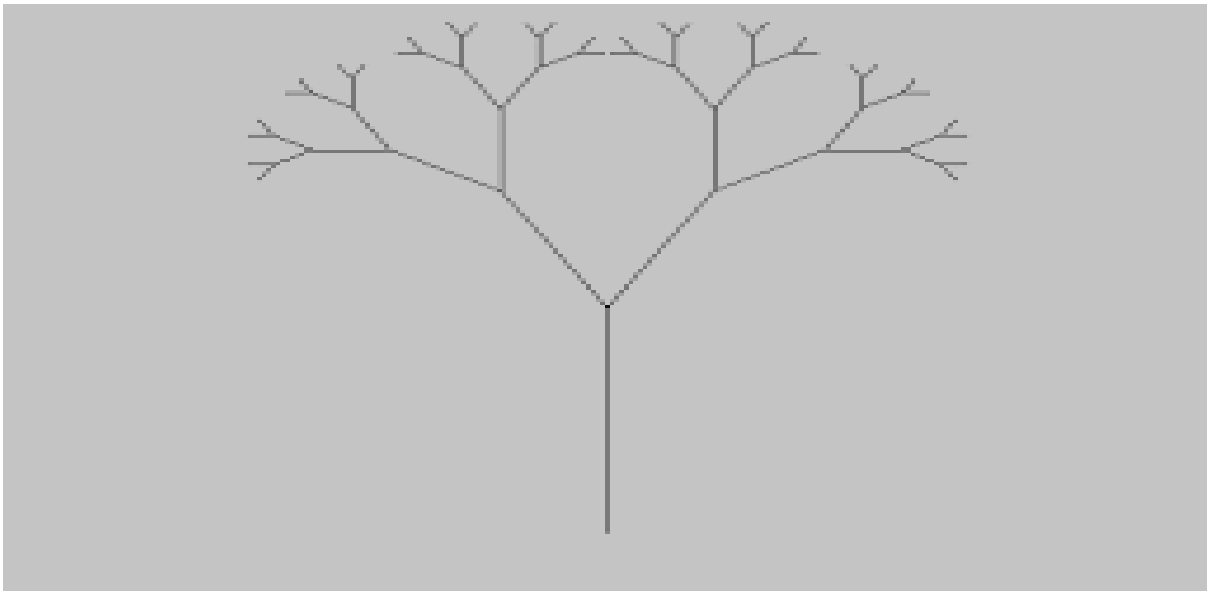

Figure 1.1: A tree as a fractal object made up of parts (branches) similar to the whole tree. Each branch looks like the whole tree.

The assumption of self-similarity across scales is the basis for the technique (Van Noordwijk *et al*., 1994). For a tree, any branching point in principle looks the same as any other, be it the first or last branching point (Van Noordwijk and Mulia, 2002). This means that it is not necessary to measure the length, diameter and taper of every single branch segment to obtain the summed volume of the whole tree (Van Noordwijk *et al*., 1994). Instead, measurements are done on a small subsample comprised of single branch segments connected from the first branching point to the terminal twig; to derive a scaling rule that expresses how diameters, lengths and tapers change throughout the canopy (Van Noordwijk and Mulia, 2002). However the self-similarity can be lost or altered below or above certain diameter thresholds, hence the rules for end structures "i.e. terminal twigs," have to be defined (Kamatou, 2003).

One method for constructing a fractal model of tree volume involves the determination of three relationships (Kamatou, 2003). The first, is the ratio of the squared diameter just below a branching point to the summed squared diameters just above the branch, (referred to as the proportionality factor "p"), as a function of stem diameter (Van Noordwijk *et al*., 1994). In principle, "p" should be approximately 1 since the cross sectional area of tracheids is approximately equal across the node (Arastu, 1998). A low co-efficient of determination when "p" is regressed against stem diameter shows the independence of the former on the latter (Van Noordwijk *et al*., 1994), and therefore establishes the viability of the fractal allometry model and validates its assumptions (Van Noordwijk and Mulia, 2002). A visual

scan of the relationship can be used to deduce the thresholds for which relationship is valid (Van Noordwijk *et al*., 1994).

The second relationship is the internode length (L) as a function of diameter at the base of that branch ($D_{proximal}$). The third required relationship, is taper per unit internode length (defined as $D_{distal}/D_{proximal}/L$), as a function of stem diameter at the base of the node (Kamatou, 2003). Determination of each relationship requires around 30 sets of measurements spread over the likely range to fit a reasonable regression model based on the normal distribution of error (Henry *et al*., 2015).

The three relationships provide the information required as input for the fractal allometry programme which calculates the volume of the whole tree. A description of how the programme works is given in Chapter 2.

Traditional forms of allometric equations and the new universal form

In biomass estimation, most allometric have a polynomial form, $Y=a+b.D+c.D^2+d.D^3$; or follow a power function, $Y=bD^a$ (Van Noordwijk, 1999).

where Y is biomass, D is diameter and; a, b, c and b are model parameters.

The shape of polynomial equations is not biologically sound and any data extrapolation outside the model range is likely to introduce significant error (Ketterings *et al*., 2001; Martin *et al*., 2010). The power function is the most used mathematical model for biomass estimation (Nickless *et al*., 2011) since it shows a good fit as it continuously rises and passes through the origin (Martin *et al*., 2010). It has also been shown to capture the allometry of a range of species (Kuyah *et al*., 2012). Colgan (2012) considers the best allometry for South African savanna trees to be that by Nickless *et al*. (2011), which follows a power-law relationship between stem diameter and above ground biomass and is of the form:

$$M = bD^a$$

where M is Above Ground Biomass (in kg), D is basal stem diameter (in cm) , b is the factor and a is the power.

Most allometric equations predict biomass from stem diameter, because stem diameter can be easily and accurately measured (West, 2009), but recent studies have shown that model fitting is greatly improved by the inclusion of additional biometric variables for example tree height either fitted independently as H or as a combined variable D^2H (Chave *et al*., 2005).

Other scholars for example, Komiyama *et al*. (2005) have also recommended including wood density as a predictive variable in biomass equations. Significant variation in form factor has been found in recent studies of diameter to height relationships and this has resulted in the drive to include both height and stem diameter in allometric equations so as to capture the variation in form factor, and also including "ρ" to account for variation in wood density (Colgan, 2012). Chave *et al*. (2005) developed an allometric equation which takes into account stem diameter (D), height (H), form factor (F) and wood density (ρ), of the form:

$$\text{Above-Ground Biomass} = F\rho(\pi D^2/4)H$$

The relationships expressed by allometric equations vary from species to species and from site to site, resulting in an inconsistent choice of the equations (Nickless *et al*., 2011). Recent approaches to estimating biomass have attempted to address the inconsistency in the choice of allometric equations by proposing universal forms of equations (Návar, 2010). The proposed universal allometric equation is a modification of Chave *et al*., (2005) equation and is of the form:

$$M = \beta_0 + \beta_1(F\rho D^2 H)$$

where M is biomass (expressed as dry mass in Mg); β_0 and β_1 are model coefficients, F is form factor, ρ is wood density (in Mg m^{-3}); D is stem diameter (m) and H is total tree height (m).

Stem diameter is traditionally measured by foresters at breast height (1.3m above the ground), thus the widely-used or mis-used abbreviation "dbh". A significant part of the tree mass may occur in the portion between the ground and breast height, and African woodland and savanna trees frequently branch quite low down. Therefore common practice in surveying African woodlands and savannas is to measure the diameter just above basal swelling, at about 0.3m above the ground. It is easier and more accurate to measure the circumference of the stem using a tape, rather than measuring diameter using a callipers, and measurements in whole cm are less prone to being incorrectly recorded than measurements in fractions of a meter. Both these factors can be subsumed into the value of β_1, and Table 1.1 shows the values of β_1 under different scenarios.

Table 1.1: Approximate theoretical values of β_1 when stem circumference is measured in metres or centimetres, as well as when diameter is calculated from a circumference measurement in m or cm

Scenario	Approximate theoretical value of β_1
Diameter measured in m	$\pi/4$ or ~0,785
Diameter measured in cm	$\pi/400$ or ~0,00785
If D was the basal circumference measured in m	$1/(4\pi)$ or ~0,08
If D was the basal circumference measured in cm	$1/(400\pi)$ or ~ 0.8×10^{-3}

The information allows for stem measurements in different units to be corrected for.

It is expected that if the diameter or height tends to zero, the mass will be zero and this means that β_0 can be ignored. The inclusion of ρ in the universal allometric equation takes out much of the parameter variation in β_1 if β_0 is ignored, meaning that β_1 should take up a value close to the theoretical values shown in Table 1.1, and should not need to be determined species by species and site by site. The wood density and form factor together capture the individuality of different species.

Due to the linear structure of the linear structure of the universal new allometry equation, all parameters (except D) contribute proportionally to the uncertainty in the answer, hence a 10% error in estimating the wood density would lead to a 10% error in mass estimation, likewise with a 10% error in the form factor or 10% error in tree height. Since D is squared, a 10% error would result in a 21% error in mass estimation. Typical mature savanna trees have a basal diameter of around 30cm and it easy to read the tape to an accuracy of 1cm. Thus the typical magnitude of D measurement error is around 1%. The typical height of a tree of that size is 10m. Heights are usually estimated by triangulation or by satellite laser altimetry, both with errors of around 0.5 to 1m, which translate into a 5 to 10% error (Rosette *et al*., 2010). While wood density can be measured in the lab with great precision to less than 1% error, the variation between individuals in a species is probably about 10%. Thus to keep the accuracy of the overall allometric estimate of mass around 10%, the form factor needs to be estimated with similar accuracy.

Form factor

The stem form factor of a tree can be defined as the ratio of its stem volume to the volume of a cylinder with a diameter equal to the basal diameter of the stem and a length equal to the height to the top of the stem (Washusen, 2002). The formula is given below:

$$F = V/(D^2H\pi/4)$$

where F is the form factor (m^3m^{-3}), V is the wood volume of the tree in m^3, D is the stem basal diameter (conceptually in m, but conventionally measured and expressed in cm), H is the height from the ground to the highest part of the stem (m).

Tree stems can be thought of as a series of cylinders, with the stem diameter and height to the top of the canopy being likened to the diameter and length of the cylinder respectively. Since the cross sectional area of the stem containing the vascular tissue is approximately equal throughout the tree (Arastu, 1998), there should be a linear relationship between the stem volume and the product of the stem cross sectional area measured near the base by the height of the tree (Burkhart and Tomé, 2012). Deviations from the ideal cylindrical stem form are expressed by the form factor. Many stems taper towards the tip, and this would lead to a form factor less than 1, whilst others may have a "coke bottle" bulge in the middle in order to provide storage volume for water, thus having a form factor greater than 1.

There are form factor theories, dating back to as early as the mid nineteenth century that have been suggested to explain both the shape of tree stems and the changes in stem diameter with an increase in tree height (Gray, 1956; Colgan *et al*., 2013) . One such is Metzger's "girder" theory, which has a mechanical basis (Gray, 1956). It suggests that the tree stem is a beam of uniform resistance against the bending force of the wind (Newnham, 1956). The lateral pressure from the wind acts on the crown and is transmitted down towards the base of the stem, resulting in the greatest pressure being felt at the base of the stem (Newnham, 1956). The tree ensures uniform resistance to the wind along its stem by allocating growth resources in response to the different pressure exerted on the different parts of the stem (Newnham, 1965). Since wind pressure decreases as we move to the upper parts of the stem, the lower parts receive more material since they are subject to the greatest wind pressure, whilst the upper parts receive relatively less material (Newnham, 1956). However the strengthening of the stem as a response to wind pressure diverts building materials from the crown and roots where they are greatly needed to ensure the growth of the tree and seed production (Newnham, 1965)**.** There is a need to optimise on the allocation of these resources

so as to ensure that the tree is able to meet its growth requirements and at the same time, have enough resources to build up enough stem strength required to withstand the wind pressure (Newnham, 1956; Colgan *et al*., 2013). The most efficient allocation of the resource material for tree growth is achieved by a decrease in stem thickness as we go up the stem (Newnham, 1956; Newnham 1965), hence the reason why trees taper.

Gray (1956) agreed with Metzger that wind pressure was the dominant factor in determining the shape of tree stems, but he disagreed with the notion that the stem was a beam of uniform resistance. In his argument, Gray (1956) suggested that the quadratic paraboloid which has 20% less volume than the cubic paraboloid (suggested by Metzger), could satisfy the mechanical requirements of the stem to resist bending from wind pressure (Newnham, 1965). Colgan *et al*. (2013) state that, "according to Metzger's theory, the height at any point along the stem is proportional to the cube of the diameter at that point". This is relatively true for the branchless part of the stem between the buttswell and the bottom of the crown (Colgan *et al*., 2013). Gray (1956) showed that for the whole tree including the branches, tree height was more closely related to the square of the diameter (Colgan *et al*., 2013). Most of the modern day form factor theories implicitly retain a mechanical basis, such as resistance to bending and elastic buckling from wind as the reasons why tree stems are shaped the way they are (Colgan *et al*., 2013).

Stem form factor is of great interest in commercial forestry which is mainly interested with the merchantable bole. Information about the shape of tree stems and how the taper of such stems varies across trees is important in the construction of volume tables for the estimation of merchantable timber (Newnham, 1965; Colgan *et al*., 2013). Tree volume models which only consider diameter at breast height (dbh) and height as the independent variables, without allowing for variations in the shape of the stem are prone to errors deriving from this source (Socha and Kulej, 2007). The modelling of tree volume began with volume tables to estimate the merchantable volume of the bole (Gervorkiantz and Olsen, 1955), and later progressed to the use of taper models (Jordan *et al*., 2005). Ver Planck and MacFarlane (2014) state that, "the next stage in tree volume modelling must be to describe the whole tree volume". Whole tree volume modelling is needed to inform the utilization of whole trees, not just the merchantable bole (Ver Planck and MacFarlene, 2014). Forest carbon accounting systems require the biomass of the whole tree to be estimated, hence the need to quantify the volume of the main stem and all the branches.

The availability of whole tree volume data makes it possible to calculate the whole tree form factor. Conceptually the form factor of a tree relates the actual wood volume of the stem and branches to the theoretical cylinder volume of the whole tree. Since this research project is focused on estimating total above ground biomass, emphasis will be on the form factor of the whole tree and not stem form factor. Without data on the form factor of a tree, the volume of a standing tree will either be under or over-estimated (Adenkule *et al*., 2013).

Relationship between form factor and other tree dimension attributes

Gray (1966) related tree form factor to the nature of branching; and found that the form factor was smaller for sparsely-branched conifers than for the heavily-branched broad-leaved trees. Trees of the same stem diameter, height and wood density can have different form factors as a result of different crown lengths and allocations to branch density (Gray, 1956). This may translate into different vertical mass distributions thereby resulting in variation in form factor that is independent of tree size (Gray, 1956; Colgan *et al*., 2013). Colgan (2012) suggested that in addition to wood density, variation in form factor between tree species was also a significant contributor to differences in tree mass. Colgan *et al*. (2013) carried out a study to determine whether form factor or wood density was the dominant driver of variation in the biomass of African savanna species of the same height and stem diameter. They concluded that variation in tree biomass amongst equal sized trees was mainly driven by variation in wood specific gravity between species. Form factors calculated by Colgan *et al*. (2013) occupied the range 0.57 to 0.77 and were not statistically different from each other for four out of the five common species: *Combretum apiculatum* (0.67±0.12) *Acacia nigrescens* (0.69±0.10), *Sclerocarya birrea* (0.70±0.18) and *Lannea schweinfurthii* (0.75±0.21).

Wood density in African savanna tree can range from about 0.4 (for example *Commiphora species*) to about 1.3Mg m^{-3} in *Combretum imberbe*, a three-fold variation (Van Vuuren *et al*., 1978). In contrast, the wood density of species documented by Colgan *et al*. (2013) ranged from 0.5 for *Sclerocarya birrea* to 1.01 for *Combretum imberbe*, a two fold variation.

Assigning tree form factor by visually assessing a tree image

The traditional approach to form factor studies is to calculate the form factor by dividing the stem volume by the volume of a cylinder that has the same diameter and length as the stem diameter and height respectively, but however an alternative method which involves assigning form factor by visually assessing a digital image of a tree, is suggested in this study. For example, a tree may be judged to be slender or squat by just inspecting its shape.

The efficiency and accuracy of such a method of assigning form factors from tree images has not been assessed to date.

A method of visually assessing bole straightness and subjectively rating tree form factor as good, fair or poor has been widely used in plantations of *Eucalyptus* and *Pinus* species, where bole straightness is important for the end use of the biomass (Shelbourne and Namkoong, 1966). In Canada, the Northern Hardwoods Research Institute assigned form factors to the trees of New Brunswick by looking at the number of stems, presence of sweeps, lean and general crown shape (Pelletier *et al*., 2013). The institute developed a tree classification system comprising of eight form classes coded F1 to F8 and for each form class there was an image of two trees which had a structure described by the form class (Pelletier *et al*., 2013). A standing tree in the field could be assigned a form factor by comparing its shape to the tree images in a handbook and selecting the tree image whose shape most closely resembles that of the standing tree.

Photo-based measurement of tree dimensions

Measurements of diameters, stem height and length of internodes can be done by felling the sample trees and measuring every single branch or by climbing the tree, but both methods are time consuming and laborious (Kamatou, 2003). Alternatively, the parameters can be estimated from dry season (leafless) photographs of the trees. This, in combination with fractal allometry could be very cost effective, but still rigorous and traceable way of deriving allometric estimates.

Advances in technology have enabled the determination tree dimension parameters by photogrammetry (Shlyakhter *et al*., 2001), which is the science of obtaining, measuring and interpreting information about the surface of an object without physical contact with the object (Schenk, 2005). Digital photogrammetry has been used in the measurement of tree dimensions, for example Zhang *et al*. (2007) estimated the fractal dimensions of tree crowns using the technique, whilst Barrett and Brown (2012) determined canopy volume from digital images. According to Barrett and Brown (2012), the use of photographs in forest mensuration speeds up the collection of data in the field without compromising on accuracy as compared to the *in situ* approach.

Takahashi *et al*. (1997) developed a photo-based measurement system for measuring tree height and diameter, comprising a special measuring camera, the MC-100, an angle sensor fitted onto the camera, an image scanner and a computer. The MC-100 has two modes; the

distance mode which measures the distance from the lens to the object it is focusing on, and the scale mode composed of a scale mark from which the size of the object is calculated by proportional allotment (Takahashi *et al*., 1997). A colour image scanner is used to enter the images into a computer with a software designed for measuring tree dimension parameters from the images (Takahashi *et al*., 1997). Under the system, tree height is calculated directly from the photograph by proportional allotment using a measuring staff of known length placed adjacent to the tree, whilst tree diameter is measured from the images by calculating the object size from the scale mark using proportional allotment (Takahashi *et al*., 1997).

Clark *et al*. (2000) estimated diameter from tree images captured by a non-metric Kodak DC-120 digital camera. The method involved determination of image pixel size and using diameter extraction software to derive diameter from raw image data for example image distance representing the stem height of the desired diameter (Clark *et al*., 2000). Shimizu *et al*. (2014) also developed a technique called digiscoping to measure the diameters of slender stems from digital images using image editing software such as Adobe Photoshop and calculations from spread-sheet software.

Chapter 2: Materials and Methods

Sites and study species

The study used a sample of eight South African tree species, seven of which collectively make up 80% of the tree biomass in the Lowveld landscape. Individuals for five of the study species, *Combretum apiculatum* (CA), *Sclerocarya birrea* (SB), *Terminalia sericea* (TS), *Dichrostachys cinerea* (DC) and *Lannea schweinfurthii* (LS), were selected at the main study site, Wits Rural Facility (24° 30'S, 31° 06'E), a 350ha teaching and research station in the central Lowveld, in Limpopo Province (Shackleton, 2001). The most common soil types at the facility are the shallow sandy lithosols which are underlain by potassic granites and grandiorite (Shackleton, 2001). The dominant tree species are *Combretum collinum*, *T. sericea*, *Acacia gerrardi*, *A. nilotica*, *D.cinearea* and *S.birrea* (Shackleton, 2001). Wits Rural Facility was chosen as the main study site as the trees occur in the vicinity and conventional empirical allometric equations exist for seven of the study species, derived at or near that location.

The second study site was an area situated between 500m and 2km east of the Phalaborwa entrance gate (22° 55'S, 31° 17'E and 350m to 450m above sea level) of Kruger National Park; where individuals of the remaining two lowveld species, *Combretum imberbe* (CI) and *Colophospermum mopane* (CM) were selected, as the two species were not found at the main study site. The area is underlain by migmatitic gneiss and is part of the Phalaborwa Sandveld dominated by *C.apiculatum, T.sericea* and *C.mopane* (Munnik *et al*., 1996).

Table 2.1: Sample sizes and the total sets of measurements for each species, as well as the locations were data were collected.

Species	Site	n	Sets of measurements
Combretum apiculatum	Wits Rural Facility	15	51
Sclerocarya birrea	Wits Rural Facility	18	53
Terminalia sericea	Wits Rural Facility	16	53
Dichrostachys cinerea	Wits Rural Facility	19	59
Lannea schweinfurthii	Wits Rural Facility	10	33
Combretum imberbe	Phalaborwa	9	37
Colophospermum mopane	Phalaborwa	13	47
Portulacaria afra	Pretoria Botanical Gardens	12	41

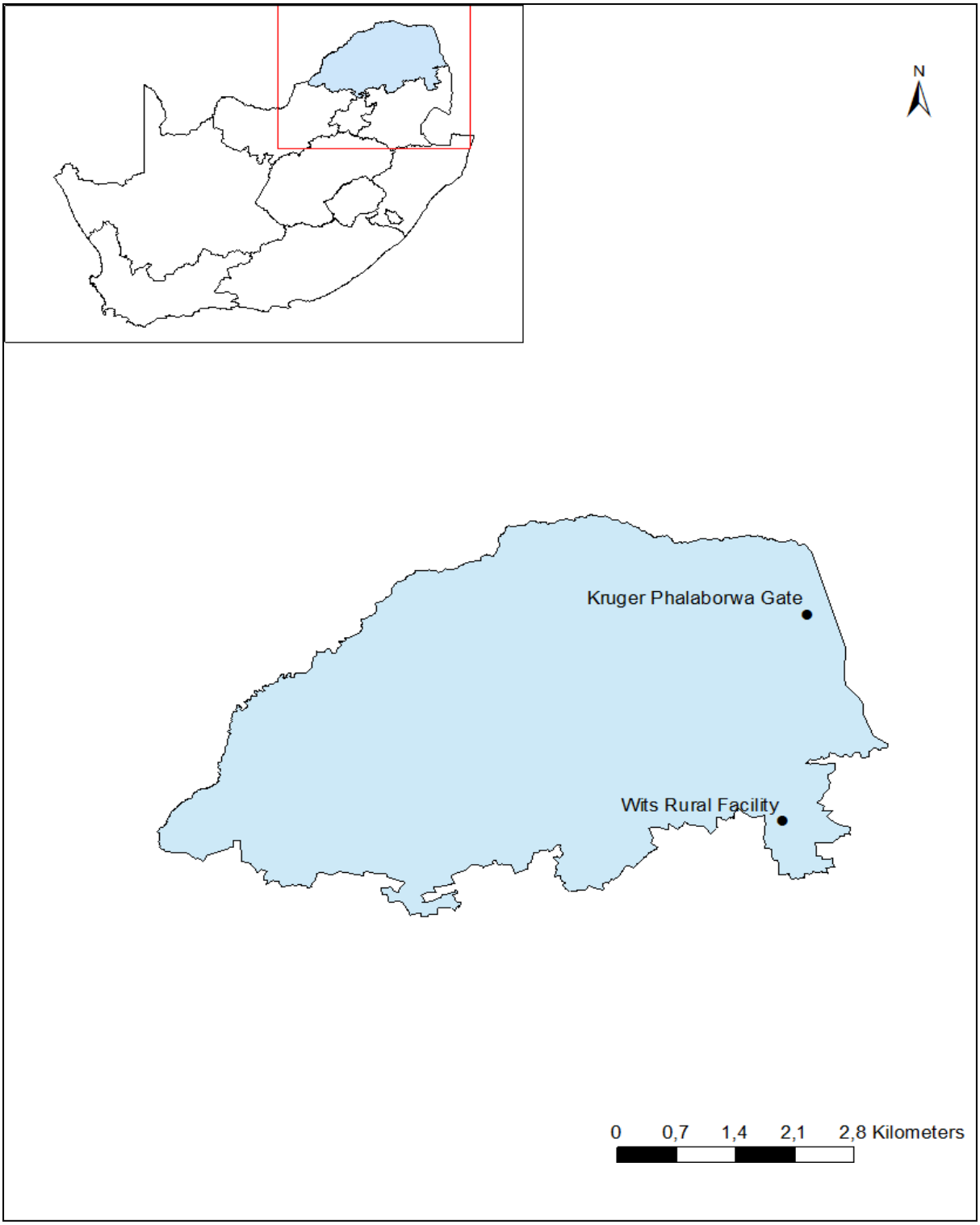

Figure 2.1: The locations of the two study sites in Limpopo Province, where data collection was done.

The eighth species, *Portulacaria afra* (PA) was selected as a deliberate example of an extreme form factor, and sample individuals were selected from the Pretoria Botanical Gardens.

The data needed to model the tree volume using fractal allometry was derived using two methods, *in situ* and in-lab measurements from images taken of the same trees in the field. Measurements at Wits Rural Facility and Phalaborwa were done in October 2015, whereas those at the Pretoria Botanical Gardens were done in December. For each method, a set of about 5 measurements for each sample tree following a branch from base to tip, was used to derive a scaling rule that expressed how diameters, lengths and tapers change throughout the canopy. Systematic sampling was done to select sample trees for each species, representative of a range of stem sizes. Each stem emerging from the ground was treated as a separate tree, thus for *D.cinerea* (a shrub species) only the single stemmed individuals were considered.

Sampling and the photography of the trees

The sample trees were chosen in such a way that a clear unobstructed photograph of each tree could be taken. A T-shaped measuring staff 2m tall and 2m wide was placed adjacent to a sample tree, vertical and perpendicular to the direction of the photograph and an image of the tree was taken using a 6 mega-pixel digital camera. The procedure was repeated for all the sample trees of each species and images were imported into IrfanView image processing software, for taking measurements. The image horizontal and vertical length of the T-shaped measuring staff were then measured in pixels, thereby enabling the calculation of the horizontal and vertical scale factor for image measurements using the formula:

Scale factor = actual length of the measuring staff (cm)/length of the measuring staff in pixels

The scale factor therefore related the actual length of the measuring staff in (cm) to the length of the measuring staff as measured on the image. The scale factor was then used to convert the image measurements from pixels into cm using the following formula:

length of tree portion (cm) = vertical scale factor × image length of tree portion (pixels)

For example, if the vertical length of the T-shaped as measured from an image was 800pixels, the scale factor of that image would be 200cm/800pixels = 0.25. This meant that for the vertical measurements on that image, each pixel was equivalent to 0.25cm on the ground. If the total height of the tree as measured on the image was 2540pixels, then the total height on the ground would be 0.25×2540 = 621.5cm. The same procedure was repeated for diameter measurements, but using a horizontal scale factor.

Procedure for data collection

Light coloured tape was wrapped around the stem at each measurement point to ensure easy visibility in the photo and to ensure that the measurements taken of the images were taken at the same place as those *in situ*. The procedure was as follows as described by Kamatou (2003):

(a) Five over-bark circumference measurements were taken using a diameter tape. The first circumference (C1) was measured just above the basal swelling, the second one (C2) just before the first branching, C3 at half basal length. The fourth (C4) and fifth circumference (C5) measurements were done on the two branches that the stem splits into just after the first branching as shown in Figure 2.1. Diameters (D1, D2, D3, D4 and D5) were calculated by dividing the circumferences (C1, C2, C3, C4 and C5) respectively by π. The length of the bole (L) from C1 to C2, and the length from the ground to C1 were measured using a tape measure.

(b) Diameters corresponding to C1, C2, C3, C4 and C5 were measured from the digital images as well using the procedure described in the previous section.

(c) About five sets of circumference and internode length measurements and measurements were taken per sample tree, both in situ and off photographs, following procedure (a) and (b), on progressive smaller branches between the first fork and the terminal branch.

(d) The total tree height was measured from images using the procedure described under the section on “Sampling and photography of trees”.

(e) Crown diameter was calculated using the cross method described by Blozan (2006). The first length measurement was from one edge of the crown through the centre of the tree to the other edge, while the second length measurement was also from edge to edge but perpendicular to the first cross section. Crown diameter was calculated as the average of the two length measurements.

(f) All of the measurements were done in cm, but measurements for the following were converted to m by dividing by 100:
height at which the basal circumference was measured, height to the first branching point, total tree height and canopy diameter.

(g) The time taken for the above measurements was noted so that comparisons could be made regarding the effort required to derive new species allometries using *in situ* and photographic approach.

(h) Two bark samples were extracted from each stem at the midpoint of each bole using an increment borer. The bark samples were then taken to the Phytotron Laboratory at the University of the Witwatersrand, where they were soaked in plastic trays for rehydration. The length and circumference of each hydrated bark sample was measured using the calliper, and the green volume was calculated using the formula:

$V = (\pi D^2 H/4)$

where V is green bark volume (in mm^3), H is the length of the bark sample (in mm), D is the circumference divided by 2 (in mm).

The bark samples were then placed in an oven for 4hours at 80°C and their oven dry weight was measured on an electric balance. Thereafter, bark density was calculated by dividing the oven dry mass of the bark samples by their green volume.

(i) The figures for the wood density for *L.shweinfurthii* and *D.cinerea* were acquired from Carson *et al*. (2012); whilst those given by Van Vuuren *et al*. (1978) for the other study species are Air dry densities (at 10% moisture content), and they were converted to wood density using the following formula:

Wood density = air dry density (at 10% moisture content)×100/(100-10%)

Van Vuuren *et al*. (1978), regarded air dry density as wood density at 10% moisture content because the average moisture content for thoroughly air dried wood in South Africa was 10.5% (which they rounded off to 10%). Likewise the researcher considers air dry density as wood density at 10% moisture content.

(j) For *P.afra*, a set of witness disks of known wet and dry diameter were used to calculate the wood density of the species. The first step was to measure the oven dry weight of each disk on an electric balance, followed by the calculation of the green volume using the formula:

$V=\pi D^2 H/4$

where V is the volume of the disk in cm^3, D is the wet diameter of the disk in cm, and H is the length of the disc (measured using a veneer calliper).

Wood shrinks tangentially, radially and longitudinally when it is oven dried, but it was assumed that longitudinal shrinkage for the disk samples was 0%. The basic density of the disk samples was calculated by dividing the oven dry weight by the green volume, and converted to air dry density (10% moisture content) by multiplying by a factor of 1.22 as suggested by Carson *et al*. (2012). The air dry density was then converted to wood density using the formula:

Wood density = air dry density (at 10% moisture content)×100/(100-10%)

The witness disks for *P.afra* did not include bark, thus it was assumed that the bark density of the species is the same as its wood density.

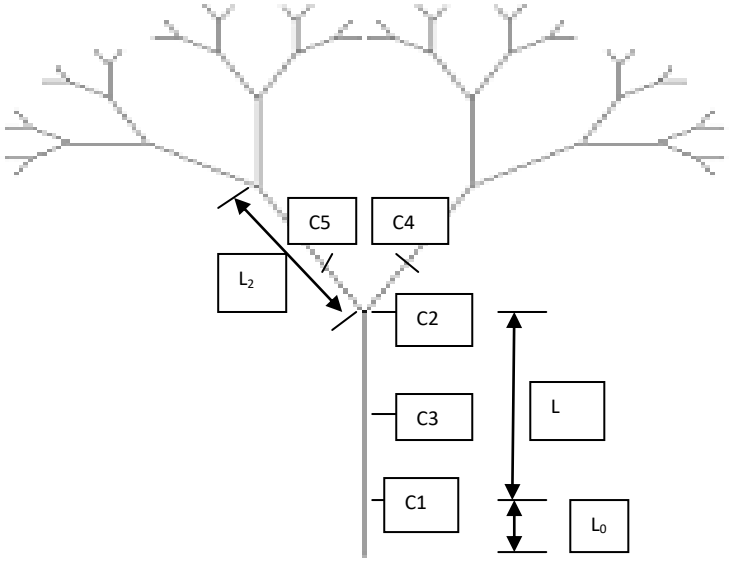

Figure 2.2: Measurements points for the collection of data needed to model tree volume based on the fractal properties of branching architecture.

Calculation of tree biomass using the Fractal allometry programme

A computer programme called FractalGu (Appendix 1), written by Professor R.J Scholes using Pascal language was used to calculate tree biomass. The programme required input files created in Notepad ("i.e. one input file for each species"), which were placed into the same computer directory as the executable file for the programme. Each input file had information about the relationships between the following (i) the ratio of the squared diameter below a branch to summed squared diameter above the branch as a function of diameter, (ii) internode length as a function of diameter at the base of that branch, (iii) taper of the stems per unit internode as a function of stem diameter, (iv) bark thickness as a function of stem diameter and (v) twig dry mass excluding leaves as a function of twig diameter. In addition to the five relationships above, each input file also had a figure for the wood density, bark density and terminal twig diameter of the species it was associated with. An example of an Input file is shown in Appendix 2.

Regression analysis was used to quantify the first three relationships for each species using data from both *in situ* and image measurements. Taper was calculated as follows:

node taper = $[100*(D_{bottom} - D_{top})/D_{bottom}]/L$

where D_{bottom} is the diameter at the base of a stem/branch segment, D_{top} is the diameter at the top of the stem/branch segment, and L is the length between the two diameters.

After reading the input file for *T.sericea* , the programme asked the researcher to enter the following input information for the first *T.sericea* sample tree: (i) a basal circumference (cm), (ii) the height above the ground at which the basal circumference was measured (m), (iii) the height at which the first branching occurred (m), (iv) the main stem circumference just below the first branch, (v) the height to the top of the tree (m) and (vi) the crown diameter (m).

Subsequently, the fractal allometry programme proceeded to calculate the volume of the whole tree by applying a recursive algorithm. The algorithm proceeded from the given diameter at the base of the tree, predicted the first internode length and taper, calculated and stored to memory the stem segment volume and then estimated the stem diameters above the node. The programme repeated the process for one branch of the fork, while putting the diameter of the other branch into temporary memory to be retrieved for later calculation. The volumes of each node were accumulated. The process ended for that branch when the predicted next diameter was smaller than the twig diameter which had been specified in the input file. The programme then went one branch back, retrieved the "other" diameter from memory and repeated the process until the terminal diameter was reached; then it went two branches back. That way, it worked its way through the entire tree, solving for the volume of all branches it left out on the way, until the whole tree volume had been calculated. Afterwards, the programme calculated the form factor for the whole tree by dividing the tree volume by the volume of the equivalent cylinder, given the basal diameter and an independent measure of tree height. After calculating the tree volume, bole volume, twig mass, bark mass, form factor and above ground tree mass of the first *T.sericea* sample tree, the programme asked the researcher to enter the input information for the second sample tree. The process was repeated until the programme calculated the above-ground biomass of all the *T.sericea* sample trees. Thereafter, the programme stopped, generated an output file for *T.sericea* and wrote it to a comma-separated variable file (CSV file).

The process was repeated for all the species, with each species having its output file. The whole process to calculate the aboveground biomass of a sample tree using the fractal allometry programme tree took fractions of a second on a modern personal computer.

Statistical analyses

Model fitting

The data violated the assumption of homogeneity of variance, which is typical of biomass data (Samalca, 2007). The solution was to log transform the data and fit a model for each species. A species neutral model was then fit by pooling data from all the trees. Log transformation resulted in the new allometry, $M = \beta_0 + \beta_1(F\rho D^2H)$ being modified into the form:

$$\ln(M) = \beta_0^* + \beta_1^* \ln(F\rho D^2H) \qquad \text{[equation 2]}$$

where M is biomass (kg), F is the form factor, ρ is wood density (kg m^{-3}), H is total tree height (m) of the tree from the ground to the top of the canopy, D is basal stem diameter (m), β_0^* and β_1^* are the log regression parameters which are estimated by ordinary least squares regression.

Comparisons of new allometry with existing empirical allometry

A biomass dataset independent of the one used in model calibration makes it possible to validate a biomass model. A model is validated by comparing its predictions with observations independent of those used to fit it (Picard *et al*., 2012). Biomass estimates from allometric models can be used to compare the models in terms of their precision, bias and parsimony using the Root Mean Square Error, 95% confidence interval of the slope and intercept of the equations, and the Akaike Information Criterion, respectively (Piccard *et al*., 2012).

Empirical allometries developed by Colgan *et al*. (2013) (Table 2.2), Nickless *et al*. (2011) (Table 2.3), and Tietema (1993) and Shackleton (1998) (Table 2.4) were chosen to be tested against the allometry developed by the researcher. Allometric equations differ between environments thus the need to test new allometry against published allometry developed from the same area. The above empirical allometries (with the exception of Tietema, 1993) were selected because they were developed in Lowveld where the research was conducted.

Table 2.2: Colgan *et al*. (2013) species-specific equations and the species neutral equation (ALL) of the form $\ln(M)=\beta_0+\beta_1\ln(D^2H)$; relating stem diameter D (cm) and height H (m) to biomass (kg).

Spp	β_0	β_1	r^2	'H' range (m)	'D' range (cm)	n
CA	-2.750	0.941	0.88	1.2-7.9	2-25	121
SB	-3.982	1.043	0.94	2.0-10.1	8-58	16
LS	-3.576	1.02	0.98	1.4-9.3	2-40	37
CM	-2.550	0.895	0.92	0.5-8.8	1-44	371
CI	-3.528	1.066	0.90	2.5-8.7	6-39	9
ALL	-2.597	0.929	0.82	0.5-15.5	2-79	707

The allometry was developed using data from 782 destructively harvested stems in a savanna woodland near Kruger National Park

Table 2.3: Nickless *et al*. (2011) species-specific equations of the form $\ln(M)=\beta_0+\beta_1\ln(D)$ relating stem diameter D (cm) to biomass (kg).

Spp	β_0	β_1	r^2	'D' range (cm)	n
TS	-3.62	2.79	0.99	0.8-10.4	36
CA	-3.27	2.8	0.98	2.1-18.2	30
SB	-3.35	2.62	0.99	3.6-33	30
CM	-2.77	2.49	0.96	1-44	30
DC	-3.08	3.12	0.95	0.7-9.6	66

Data sets used in the regression statistics were made available by Scholes (1988) and Goodman (1990)

Table 2.4: Species-specific equations by Tietema (1993) and Shackleton (1998) expressed in the original form $\ln(M)=b+a\ln(D^2H)$; relating stem diameter D (cm) and height H (m) to biomass (kg). The original form was also converted to the standard form $M=bD^a$; relating stem diameter (cm) to biomass (kg); where "b" is the factor and "a" is the power

Author	spp	Original form: $\ln(M)=b+a\ln(D^2H)$;		r^2	n	Standard form: $M=bD^a$;	
Shackleton (1998)		a (slope)	b (intercept)			a (power)	b (factor)
	TS	2.687	-2.827	0.98	15	2.687	0.032273
	DC	2.559	-2.571	0.96	15	2.559	0.050258
Tietema (1993)	TS	1.2286	0.0871	0.95	12	2.4572	0.032366
	CA	1.1001	0.2232	0.94	58	2.2002	0.085556
	CM	1.3341	0.0644	0.95	36	2.6681	0.023329
	DC	1.0337	0.2787	0.85	33	2.0674	0.108558

A major limitation of this study was the unavailability of an independent biomass data to validate the new allometry. The unavailability of an independent dataset meant that there were no biomass estimates for the new allometry form, and this made it impossible to compare the new allometry with existing empirical allometry in terms of precision and parsimony.

The first option was to express both the new and empirical allometry in the standard form $M=bD^a$, by relating biomass (M in kg) to the basal stem diameter (D in cm), and proceed to do a graphical exploration of the equations. However not much can be deduced from graphically comparing the equations in the above mentioned form, thus the next step was a comparison using the 95% confidence interval of the slope and intercept of the allometric equations. The allometry by Tietema (1993) and Shackleton (1998) was in the original form $\ln(M)=b+a\ln(D^2H)$, but the constants "b" and "a" were changed to β_0 and β_1 respectively, so that all the equations would have the regression co-efficients. A major problem was that the new allometry and the empirical allometries had different predictor variables, i.e. $F\rho D^2H$ (for the new allometry), D (for Nickless *et al*., 2011) and D^2H [for Tietema (1993); Shackleton (1998) and Colgan *et al*. (2013)]. The solution was to express the empirical equations in the untransformed form $M = \beta_0 + \beta_1(F\rho D^2H)$. The empirical equations by Tietema (1993); Shackleton (1998) and Colgan *et al*. (2013) were converted from $\ln(M) = \beta_0^*+\beta_1^*\ln(D^2H)$ to the form:

$$M = \beta_0 + \beta'_1(D^2H) \qquad \text{[equation 3]}$$

where F and ρ were subsumed in the meta-constant β'_1

Equations by Nickless *et al*. (2011) were converted from $\ln(M) = \beta_0^*+\beta_1^*\ln(D)$ to the form:

$$M = \beta_0 + \beta'_1(D) \qquad \text{[equation 4]}$$

where F, ρ and H were subsumed in the meta-constant β'_1

Data on form factors (estimated from the fractal allometry programme) and wood density (calculated according to the methodology given under point (i) of the section on "Procedure for data collection") made it possible to split the meta-constant (β'_1) of equation 3 into its components β_1, F and ρ. The meta-constant (β'_1) of equation 4 was split into its components β_1, F, ρ and H using data from form factors, wood density and total tree height (measured from images as described in the previous section of this chapter). This is made it possible to

express equations 3 and 4 in the form $M = \beta_0 + \beta_1(F\rho D^2H)$. Thereafter, the empirical equations were log-transformed into the standard form $\ln(M) = \beta_0^* + \beta_1^* \ln(F\rho D^2H)$, by regressing the logarithm of biomass (M) to the logarithm of the compound variable ($F\rho D^2H$). The new allometry and the standard form of empirical allometry were now of the same equation form, making it possible to test the former against the latter. The 95% confidence interval of the slope and intercept of the equations were calculated as follows:

95% Confidence interval of slope = $\beta_1^* \pm$ (SE of slope $\times t_{1-\alpha/2, n-2}$) [equation 5]

and

95% Confidence interval of intercept = $\beta_0^* \pm$ (SE of intercept $\times t_{1-\alpha/2, n-2}$) [equation 6]

where β_0^* is the intercept, β_1^* is the slope, SE is the standard error computed by SPSS, $t_{1-\alpha/2}$ is the 1- α /2 quantile of the standard t-distribution, α is 0.05, n is the sample size, n-2 is the degrees of freedom.

To test if the inclusion of form factor in allometric equations improves the precision of biomass estimation, a log-log model relating the compound variable (ρD^2H) to the biomass estimated from the best empirical allometry by Colgan *et al*. (2013) was fit.

Throughout the analyses, checks were performed to ensure that the assumptions of normality of residues and homogeneity of variance were not violated. Statistical analysis was performed using SPSS 16.0 (2010) at 95% confidence limits.

Trend analysis for form factors

Principal component analysis (PCA) was run in XLSTAT (2015.1) using the following variables; form factor, taper ratio, form quotient (ratio of the diameter above breast height to diameter at breast height), crown width, wood density, basal stem diameter and height. The purpose of PCA is to identify and explain trends in a data set, thus trends in the form factors of the study species were explored using PCA. Normalized versions of the original variables were supplied to the principal components because the variables were on different scales. The two principal components with the highest eigenvalues were chosen as the axis for an ordination plot on which the trends for form factors would be assessed.

Chapter 3: Results

Comparisons of regression formulae derived from *in situ* and image measurements

Species specific regression formulae for the fractal allometry programme were derived from 112 trees over a range a size classes. A comparison of stem diameters and node lengths measured *in situ* and from images shows that the image measurements underestimated both parameters by 4% and 5%, respectively (Figure 3.1).

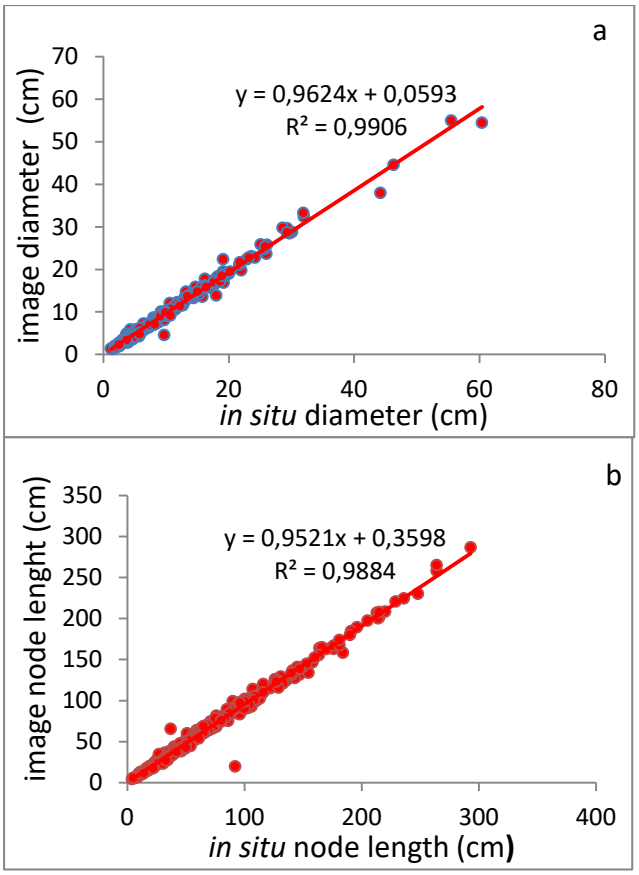

Figure 3.1: *In situ* versus image measurements of stem diameter (a) and node length (b).

Statistical tests were used to test if the branch ratio, taper ratio and node length differed by species and or method, and to assess the significance of the slope and intercept of the different regression formulae. According to the ANOVA results each variable differed by species ($p<0.001$), but not by method used; with p values of 0.294, 0.236 and 0.383, respectively for branch ratio, taper ratio and node length. All the interaction effects (species×method, species×diameter, method×diameter and species×method×diameter) were not statistically significant for the relationships between branch ratio and stem diameter

(Table 3.1), branch taper and stem diameter (Table 3.2) and node length and stem diameter (Table 3.3).

The co-efficient of determination for all the relationships was very low for all the species with $0.0001<r^2<0.093$ (in situ) and $0.02< r^2<0.129$ (images) for the relationship between branch ratio and stem diameter, $0.007<r^2<0.205$ (in situ measurements) and $0.029<r^2<0,246$ (image measurements) for branch taper and stem diameter, and $0.097< r^2<0.352$ (in situ) and $0.128< r^2<0.206$ (images) for node length and stem diameter (Appendices 3.1, 3.2 and 3.3).

For the relationship between branch ratio and stem diameter, the slopes for equations derived from *in situ* measurements were not statistically different from zero for all the species, with $0.213<p<0.806$ (Appendix 3.1), which means that branch ratio is not a function of stem diameter for *in situ* measurements. As for image measurements, the slope for the equations for *C.imberbe* ($p=0.045$) and *D.cinerea* ($p=0.034$) was statistically different from zero, implying that branch ratio is a function of stem diameter for the two species, but for the other species the slope was not statistically different from zero, with $0.138<p<0.769$ (Appendix 3.1). The intercept was statistically different from zero for all the species regardless of the method used, with $p<0.001$ for all the equations (Appendix 3.1).

The slopes of the equations for the relationship between branch taper and stem diameter were not statistically different from zero for *D.cinerea*, *L.shweinfurthii*, *C.mopane* and *C.imberbe* with $0.072<p<0.526$ (in situ) and $0.058<p<0.709$ (images); but different from zero for the other four species, *T.sericea*, *C.apiculatum*, *S.birrea* and *P.afra*, with $p<0.005$ and $p<0.03$ for equations from *in situ* and image measurements respectively (Appendix 3.2). The intercept was statistically different from zero for equations derived using both methods with $p<0.001$ for all the equations.

For the relationship between node length and stem diameter, the slopes of the equations for *T.sericea*, *D.cinerea*, *L.shweinfurthii*, *C.mopane* and *C.imberbe* were not significant, with $0.093<p<0.909$ and $0.064<p<0.863$ (Table 3.3) for *in situ* and image measurements respectively. The equations for the other species, *C.apiculatum*, *S.birrea* and *P.afra*, had slopes that were statistically significant $p<0.048$ (*in situ* measurements) and $p<0.021$ (image measurements).

The relationship between bark thickness and stem diameter was strong for *T.sericea*, *C.apiculatum*, *S.birrea* and *C.imberbe* ($p>0.504$), weak for *L.schweinfurthii* ($p=0.3$) and very

weak for *D.cinerea* and *C.mopane* ($p<0.054$). The slope of the regression formula was significant for *T.sericea* and *D.cinerea* ($p<0.005$) and not significant for the other species with $0.301<p<0.838$). Bark thickness was also shown not to vary with species ($p=0.521$).

Time required to collect allometric data

Data was collected over a period of 16 days, which translates into an average of two days per species. Each day, nine trees were measured *in situ* over eight hours, the period also included the time taken to move from tree to tree. It took an average of 30 minutes per tree to collect the fractal data using *in situ* measurements. An average of one hour was spent collecting fractal data using the image analysis approach. The period included the time taken to climb each tree and wrap coloured tape around the stem at each measurement point, capturing the image, importing the image into IrfanView image processing software and measuring the diameters and node lengths.

Table 3.1: ANOVA results for the relationship between branch ratio and stem diameter (cm)

Source	Type III Sum of Squares	df	Mean Square	F	p
Corrected Model	18.294[a]	670	0.027	1.331	0.058
Intercept	820.061	1	820.061	218.338	0.000
Species	0.895	7	0.128	6.236	0.000
Method	0.023	1	0.023	1.118	0.294
Diameter	7.440	271	0.027	1.339	0.065
species×method	0.084	6	0.014	0.681	0.665
species×diameter	6.489	239	0.027	1.324	0.075
method×diameter	1.172	67	0.017	0.853	0.747
species×method×diameter	0.037	9	0.004	0.201	0.993
Error	1.579	77	0.021		
Total	1078.187	748			
Corrected Total	19.873	747			

R Squared = 0.921 (Adjusted R Squared = 0.229)

Table 3.2: ANOVA results for the relationship between branch taper and stem diameter (cm)

Source	Type III Sum of Squares	df	Mean Square	F	p
Corrected Model	552.195[a]	646	0.855	1.215	0.156
Intercept	2396.410	1	2396.410	68.411	0.000
Species	18.943	7	2.706	3.846	0.001
Method	1.006	1	1.006	1.431	0.236
Diameter	261.043	264	0.989	1.405	0.047
species×method	3.384	6	0.564	0.802	0.572
species×diameter	137.046	231	0.593	0.843	0.823
method×diameter	35.770	65	0.550	0.782	0.840
species×method×diameter	0.702	6	0.117	0.166	0.985
Error	48.546	69	0.704		
Total	3334.417	716			
Corrected Total	600.740	715			

R Squared = 0.919 (Adjusted R Squared = 0.163)

Table 3.3: ANOVA results for the relationship between node length (cm) and stem diameter (cm)

Source	Type III Sum of Squares	df	Mean Square	F	p
Corrected Model	403.395[a]	670	0.602	1.766	0.001
Intercept	9571.291	1	9571.291	153.257	0.000
Species	39.250	7	5.607	16.445	0.000
Method	0.262	1	0.262	0.769	0.383
Diameter	121.507	271	0.448	1.315	0.077
species×method	0.381	6	0.064	0.186	0.980
species×diameter	109.926	239	0.460	1.349	0.062
method×diameter	17.336	67	0.259	0.759	0.875
species×method×diameter	3.482	9	0.387	1.135	0.349
Error	26.254	77	0.341		
Total	12391.754	748			
Corrected Total	429.649	747			

R Squared = 0.939 (Adjusted R Squared =0.407)

Table 3.4: ANOVA results for the relationship between bark thickness (mm) and stem diameter (cm)

Source	Type III Sum of Squares	df	Mean Square	F	p
Corrected Model	7.893[a]	97	0.081	1.247	0.548
Intercept	13.328	1	13.328	204.306	0.005
Species	0.293	4	0.073	1.124	0.521
stemD	6.019	88	0.068	1.048	0.611
species×stemD	0.226	3	0.075	1.157	0.495
Error	0.130	2	0.065		
Total	22.459	100			
Corrected Total	8.024	99			

R Squared = 0.984 (Adjusted R Squared = 0.195)

Model fitting

Species specific allometry was constructed from 112 trees, whose diameter and height ranges were 4 to 89cm and 0.8-15.9m respectively. All the species specific allometries had good fits with $0.93<r^2<0.99$ and a species neutral equation was derived for all the study the species (Table 3.5). Graphs of the species-specific allometries developed by the researcher are shown in Figure 3.2.

Table 3.5: Species-specific biomass allometric equations, relating form factor, field wood density (kg/m^{-3}), basal stem diameter (m) and height (m) to biomass (kg).

spp	β_0^*	SE of β_0^*	β_1^*	SE of β_1^*	r^2	F $\mu\pm\sigma$	ρ $\mu\pm\sigma$	'H' range (m)	'D' range (cm)	n
TS	0.103	0.125	0.912	0.027	0.98	0.48±0.13	823±62	2.5-9.5	5-42	16
CA	-0.318	0.162	1.017	0.042	0.97	0.62±0.11	949±51	2.8-7.2	5-18	15
SB	0.127	0.113	0.909	0.025	0.98	0.50±0.11	566±27	3.1-15.9	7-89	18
DC	-0.210	0.104	0.980	0.038	0.97	0.69±0.14	697±72	2.4-5.8	4-24	19
LS	0.132	0.148	0.925	0.027	0.99	0.51±0.12	530±17	4.0-10.3	17-80	10
CM	0.275	0.231	0.880	0.050	0.96	0.43±0.10	1027±48	4.2-10.4	12-28	13
CI	1.038	0.274	0.786	0.045	0.97	0.63±0.14	1235±5	4.7-11.5	15-38	9
PA	-0.133	0.112	0.875	0.071	0.93	0.69±0.19	340	0.8-3.7	4-19	12
ALL	-0.121	0.042	0.962	0.010	0.98	0.57±0.16	753±256	0.8-15.9	4-89	112

TS (*Terminalia sericea*), CA (*Combretum apiculatum*), SB (*Sclerocarya birrea*), DC (*Dichrostachys cinerea*), LS (*Lannea Schweinfurthi*), CM (*Colophospermum mopane*), CI (*Combretum imberbe*), PA (*Portulacari afra*). The last row (ALL) shows the species neutral equation. Species-specific models are of the form $\ln(M)=\beta_0^* + \beta_1^*\ln(F\rho D^2H)]$, β_0^* and β_1^* are log regression coefficients, SE is the standard errors for the coefficients, R^2 is the co-efficient of determination, F is the form factor (mean $\mu\pm$standard deviation σ), ρ is field wood density (mean $\mu\pm$standard deviation σ), H is total tree height (m), D is basal stem diameter (m) thought the range in the table is given in cm, and n is sample size.

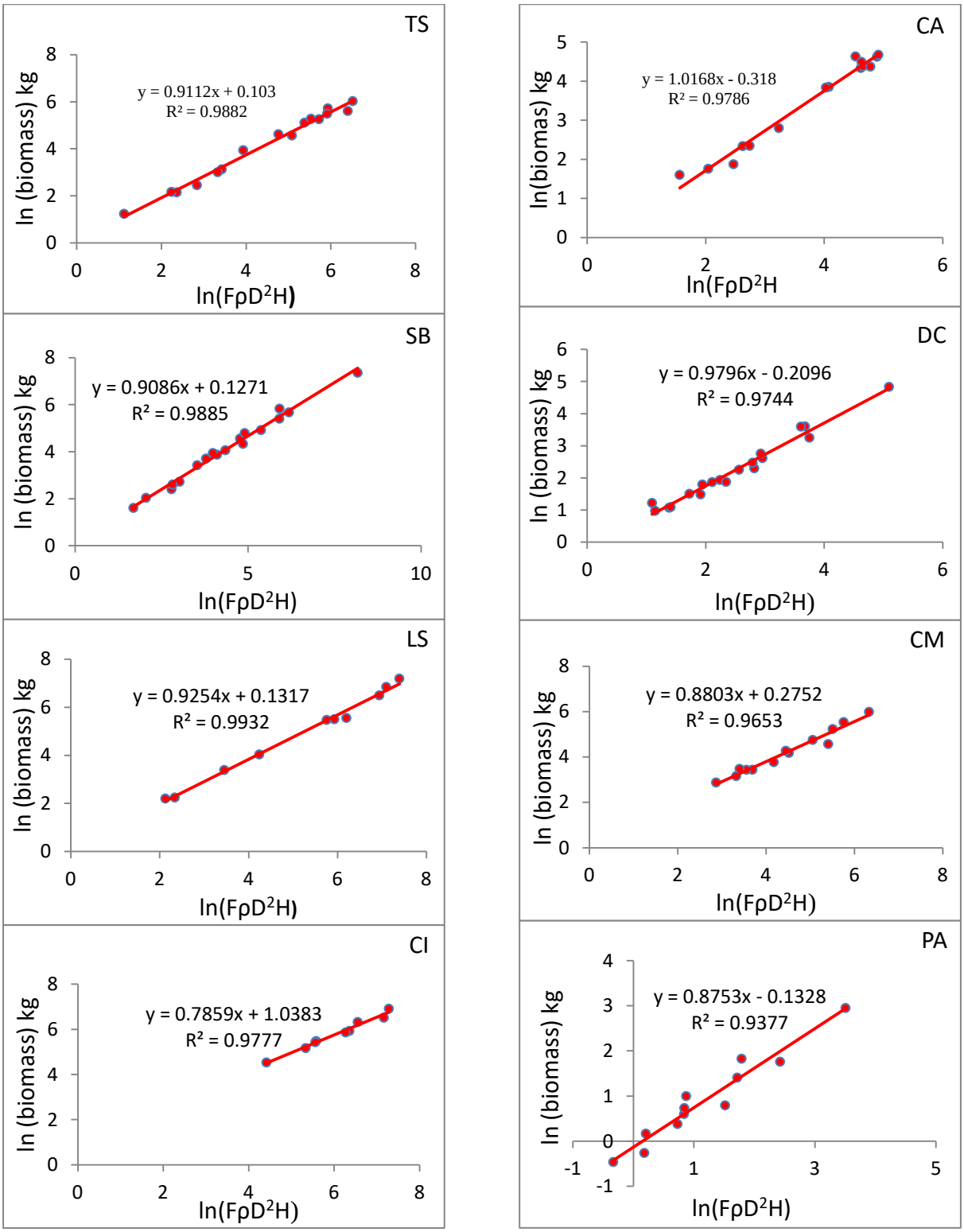

Figure 3.2: Researcher's species-specific equations relating the logarithm of biomass (kg) to the logarithm of the compound variable ($F\rho D^2H$). Each point represents a tree stem.

Researcher's vs Colgan *et al*. (2013) form factors

The form factors estimated by the fractal allometry were lower for each species as compared to those reported by Colgan *et al*. (2013), with margins as high as 0.3, 0.25 and 0.2 for *T.sericea*, *L.schweinfurthii* and *S.birrea* respectively, and as low as 0.05 for *C.apiculatum* (Table 3.6). *C.mopane* had the lowest form factor for both authors, 0.43 (Researcher) and 0.57 (Colgan *et al*., 2013), respectively.

Table 3.6: Comparisons between form factors derived by the researcher and those by Colgan *et al*. (2013).

Spp	Researcher's form factor $\mu\pm\sigma$ (n)	Colgan *et al*. (2013) form factor $\mu\pm\sigma$ (n)
TS	0.48±0.13 (16)	0.77±0.18 (12)
CA	0.62±0.11 (15)	0.67±0.12 (6)
SB	0.50±0.11 (18)	0.70±0.18 (9)
DC	0.69±0.14 (19)	---
LS	0.51±0.12 (10)	0.75±0.21 (6)
CM	0.43±0.10 (13)	0.57±0.12 (25)
CI	0.63±0.14 (9)	0.72±0.29 (4)
PA	0.69±0.19 12)	---
ALL	0.57±0.16	0.67±0.29 (69)

All shows the species mean form factor, μ is mean and σ is standard deviation. The number of trees per species whose form factors were calculated is given in brackets (n). (---) mean that Colgan *et al*. (2013) did not calculate the form factor of that species.

Comparisons between equations

Model coefficients for the new and empirical allometry in the form (M) = $\beta_0^*+\beta_1^*\ln(F\rho D^2H)$ and $M=bD^a$ are given in Appendix 3.1 and 3.2 respectively. A graphical comparison of the new equations and empirical equations of the form $M=bD^a$ is shown in Figure 3.3. However not much could be deduced by comparing the equations in the form $M=bD^a$. Instead the equations were compared in their standard form $\ln(M)=\beta_0^*+\beta_1^*\ln(F\rho D^2H)$ and a contrast of the 95% confidence intervals of the slope and intercept of the regression equations is shown in Figures 3.4 and 3.5.

The slopes and intercepts of the equations in the form $\ln(M)=\beta_0^*+\beta_1^*\ln(F\rho D^2H)$ for the researcher's allometry equations were different from those of the empirical types, as denoted by the × note in Table 3.7, with a few exceptions, denoted by a tick✓. Notable amongst the

exceptions were the slope and intercept for the researcher's equations for *C.apiculatum* and *C.mopane* which were similar to those given by Nickless *et al*. (2011) as the confidence intervals overlapped. Colgan *et al*. (2013) allometry had the narrowest 95% confidence interval for each species (except *D.cinerea*, which was not part of that study). There was overlap between the confidence intervals of the slopes and intercepts of the species neutral equation of Colgan *et al*. (2013) and the researcher's allometry for *T.sericea*, *S.birrea* and *L.schweinfurthii*. The researcher's species specific and neutral allometry was also found to be different.

For each species the biomass calculated by the fractal allometry program differed greatly from the estimates of the empirical allometry for the bigger trees, as diameters of those bigger trees were outside the range of validity of the former (Figure 3.3). Biomass calculated by the program was lower as compared to that calculated using Colgan *et al*. (2013) and Nickless *et al*. (2011) equations, meaning that the new allometry will provide lower biomass estimates as compared to the empirical allometry.

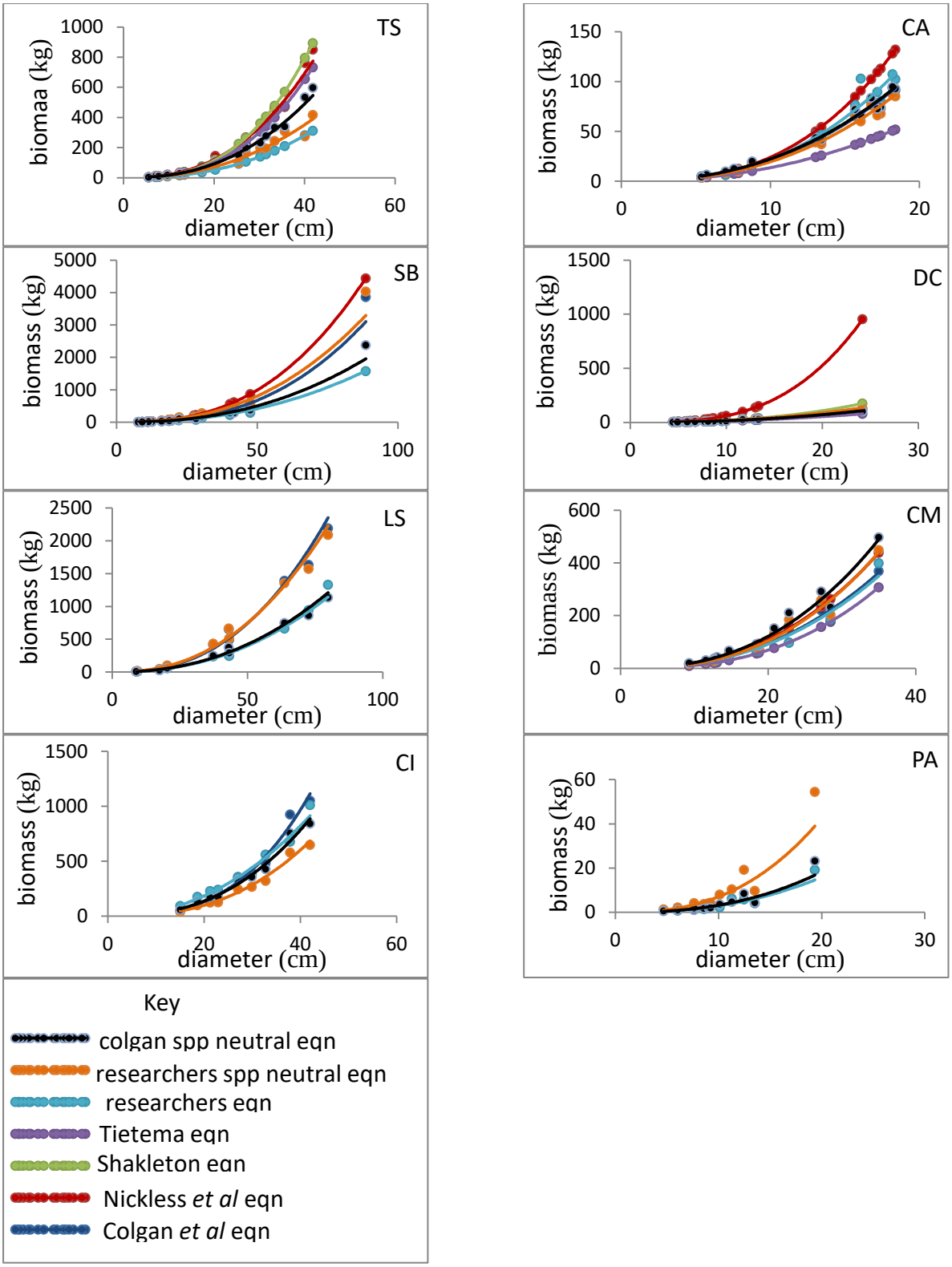

Figure 3.3: Comparisons of the standard form ($M=bD^a$) of the new allometry and empirical allometry.

Table 3.7: Comparisons of the slope and intercept of the equations derived from fractal allometry to that of empirical allometries by the different authors. The equations are of the form $\ln(M)=\beta_0^* + \beta_1^* \ln(F\rho D^2 H)$

spp	component	Colgan *et al.* (2013)	Nickless *et al.* (2011)	Shakleton (1998)	Tietema (1993)	Researcher spp general equation	Colgan *et al.* (2013) spp general equation
TS	slope	×	×	×	✓	×	✓
	intercept	✓	×	×	×	×	✓
CA	slope	×	✓	---	×	×	×
	intercept	×	✓	---	✓	×	×
SB	slope	×	×	---	---	×	✓
	intercept	×	✓	---	---	×	✓
DC	slope	---	×	×	×	✓	×
	intercept	---	×	✓	×	×	×
LS	slope	×	---	---	---	×	✓
	intercept	×	---	---	---	×	✓
CM	slope	×	✓	---	✓	×	×
	intercept	×	✓	---	---	×	×
CI	slope	×	---	---	---	×	×
	intercept	×	---	---	---	×	×
PA	slope	---	---	---	---	✓	×
	intercept	---	---	---	---	×	×

A tick (✓) shows that the slope/intercept of the fractal equation is similar to that of another author, an (×) mark shows a difference. For example a tick (✓) for the slope of the CA equation by Nickless *et al*. (2011) means that the slope for the researchers equation for *C.apiculatum* is similar to that of the Nickless *et al*. (2011) for the same species. Two slopes or intercepts are considered similar if their error bars overlap (see Figure 3.4 and3.5). (---) shows that there is no empirical allometry for that species by that author.

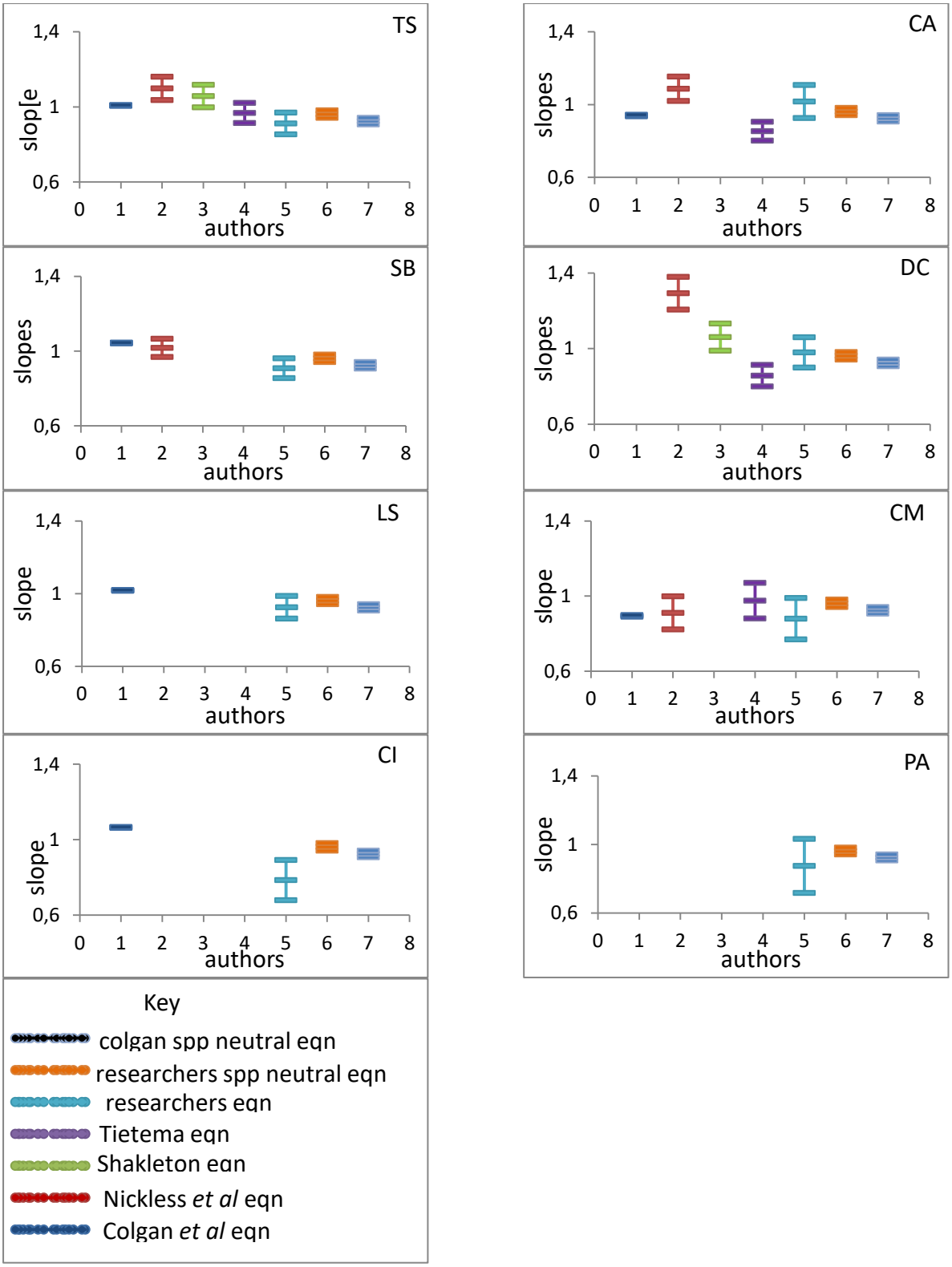

Figure 3.4: The 95% confidence intervals of the slope of the standard equation form $\{\ln(M) = \beta_0^* + \beta_1^* \ln(F\rho D^2H)\}$ for the species specific and species neutral new allometry, empirical allometry and the Colgan *et al.* (2013) species neutral allometry.

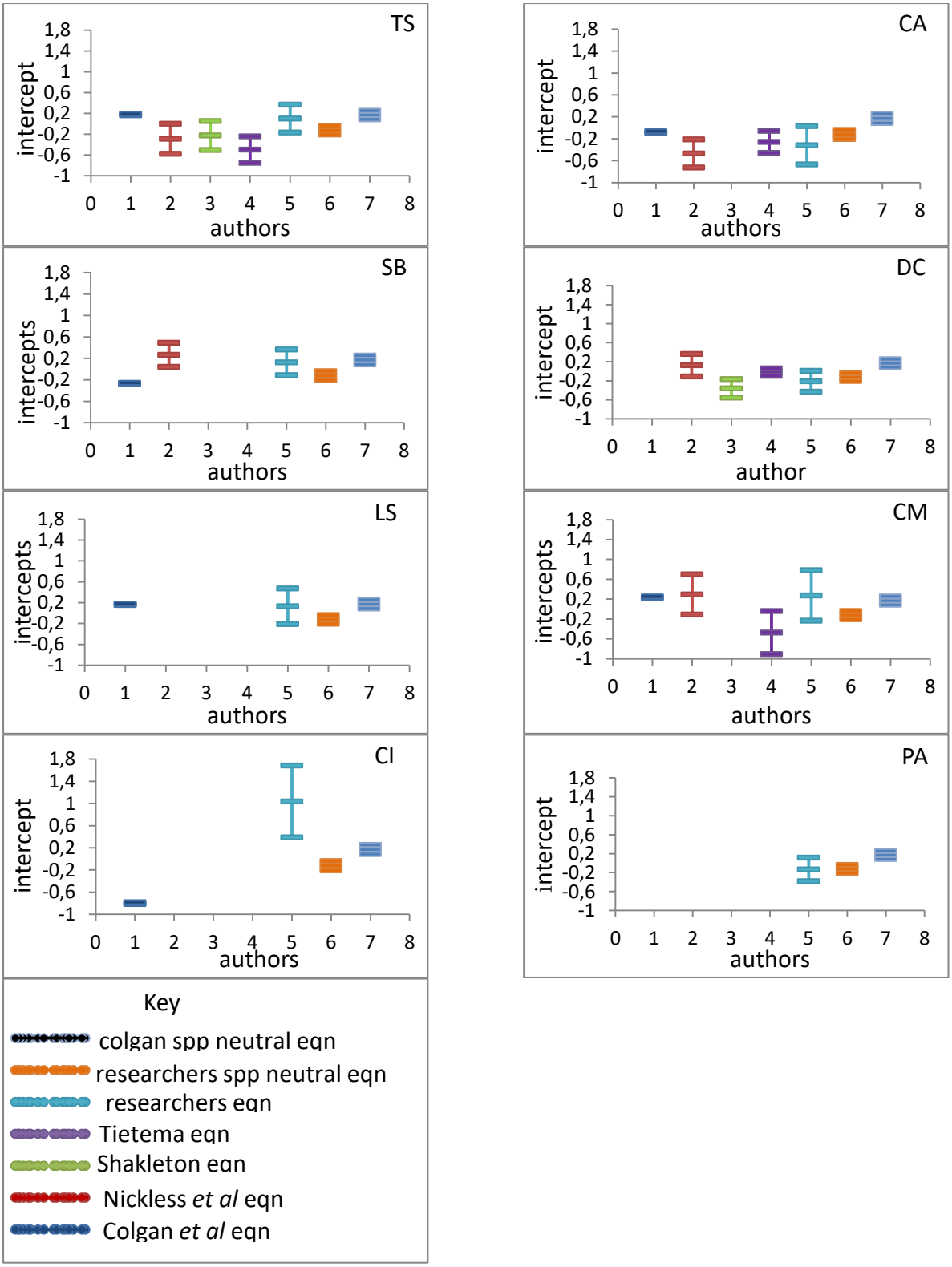

Figure 3.5: The 95% confidence intervals of the intercept of the standard equation form $\{\ln(M) = \beta_0^* + \beta_1^* \ln(F\rho D^2 H)\}$ for the species specific and species neutral new allometry, empirical allometry and the Colgan *et al.* (2013) species neutral allometry.

Effect of form factor on model precision

A log-log model relating the compound variable (ρD^2H) to the biomass estimated from the best empirical allometry by Colgan *et al*. (2013), showed that the slopes were from 0 to 11% less than 1, meaning that including form factor improves the accuracy in biomass estimation by 11% (Figure 3.6).

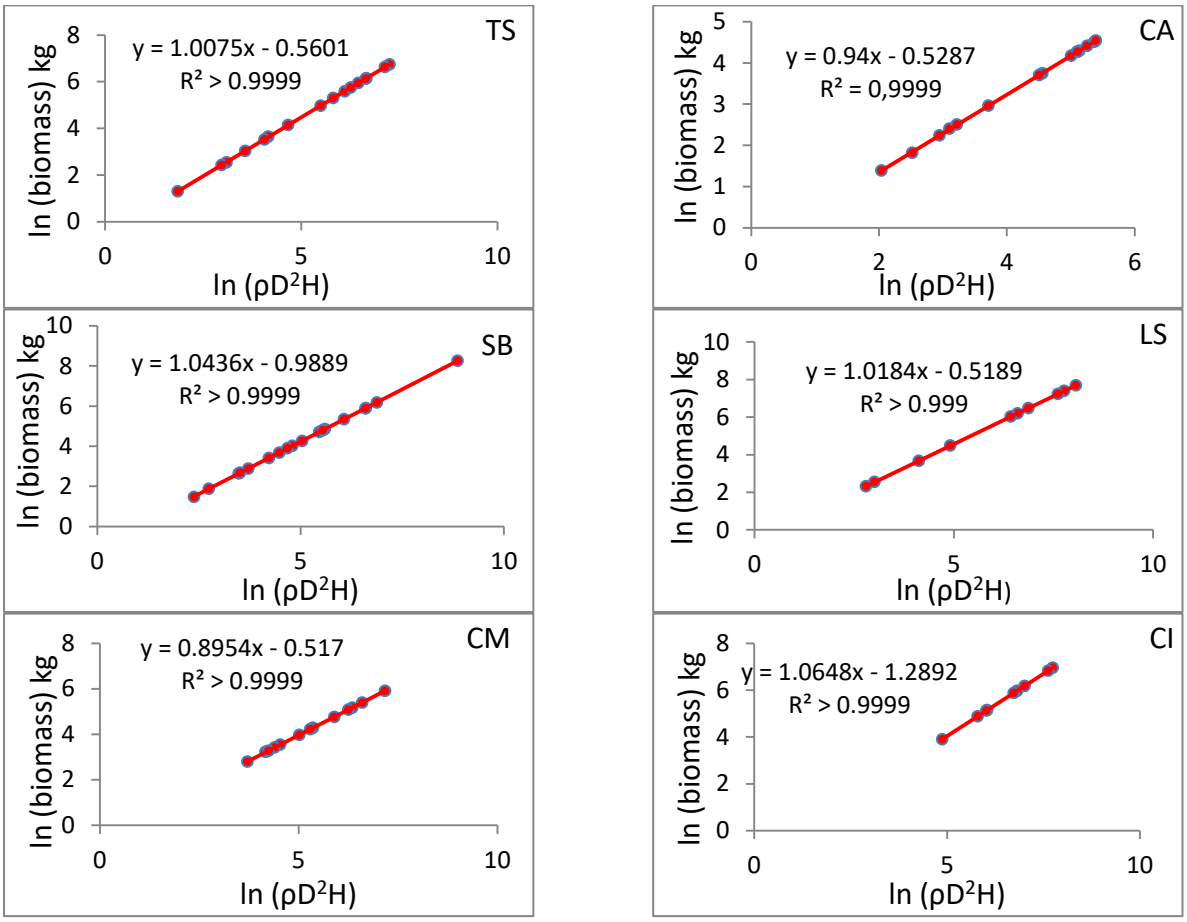

Figure 3.6: Species specific equations relating the logarithm of biomass (kg) as estimated from the Colgan *et al*. (2013) equation for that species, to the logarithm of the compound variable (ρD^2H).

Form factor and its correlation with the other predictor variables

Species mean form factors ranged from 0.43 to 0.69, with an overall mean of 0.57 (Table 3.5). There was interspecific variation in form factor as shown by the distribution of form factors of each species in different quadrants in Figure 3.6, though further statistical tests revealed that the variation was not statistically significant p=0.579 at 5% level (Table 3.8).

Table 3:8: ANOVA results showing how the form factors varied by basal stem diameter and species

Source	Type III Sum of Squares	Df	Mean Square	F	p
Corrected Model	2.869[a]	109	0.026	3.655	0.239
Intercept	33.658	1	33.658	93.9	0.000
Species	0.027	7	0.007	0.924	0.579
Diameter	1.828	101	0.018	2.513	0.327
Species×Diameter	0.002	1	0.002	0.347	0.615
Error	0.014	2	0.007		
Total	39.375	112			
Corrected Total	2.883	111			

a. R Squared = 0.995 (Adjusted R Squared = 0.723)

Form factor was negatively correlated with all the other predictor variables, with Pearson Correlation coefficients of -0.177, -0,547, and -0.649 for the linear relationships between form factor and wood density, form factor and basal diameter and, form factor and height; respectively. Only the relationship between form factor and wood density was statistically significant (p=0.031) at 5% level. Wood density was positively correlated with both basal diameter and height (r=0.085 and 0.477, respectively) but both relationships were not statistically significant at 5% level.

Table 3.9: Correlation amongst the predictor variables**,** with significance at 1% and 5% level, representing by * and ** respectively, where r is the Pearson r correlation coefficient

		form factor	wood density	diameter	height	mean	Range
form factor	r	1	-0.177*	-0.547**	-0.65**	0.571	112
	Sig. (1-tailed)		0.031	0.000	0.000		
	N	112	112	112	112		
wood density	r	-0.177*	1	0.085	0.477**	753.9	112
	Sig. (1-tailed)	0.031		0.187	0.000		
	N	112	112	112	112		
diameter	r	-0.547**	0.085	1	0.819**	0.196	112
	Sig. (1-tailed)	0.000	0.187		0.000		
	N	112	112	112	112		
height	r	-0.649**	0.477**	0.819**	1	5.65	.477**
	Sig. (1-tailed)	0.000	0.000	0.000			
	N	112	112	112	112		

Pattern analysis of form factors

Two principal components, F1 and F2 with the highest eigenvalues (Table 3.10), were chosen as the axis for a map on which the trends for form factors would be assessed. The F1 and F2 axis were closely related with tree height and form quotient, respectively; with each axis explaining 55.6% and 17.9% of the variation in form factor, in that order (Table 3.10).

The distribution and clustering of form factors is shown in Figure 3.7. In the upper left quadrant, *S.birrea* form factors are clustered near the intersection of the F1 and F2 axis, though many of the dots are distributed along the F1 axis, whilst some degree of clustering is observed for *T.sericea* along the F2 axis and for *P.afra* near both axes. Form factors for half the *T.sericea* trees are also clustered in the upper right quadrant, and in the same quadrant, there is also a cluster of form factors of *S.birrea* and *L.schweinfurthii* trees. There is a cluster of form factors for *D.cinerea* and *C.mopane* along or near the F2 axis in the lower left and right quadrants respectively. Form factors for half the number of *C.apiculatum* trees are distributed in both the lower left and lower right quadrants, even though there is no clustering for the species.

Trees of high form factors ranging (0.73 to 1.1) are mainly distributed along the F2 axis in the lower parts of the lower right and left quadrants, with the exceptions of high form factors for *P.afra* which are distributed in the upper left quadrant. On the other hand, the upper and lower portions of the upper right quadrant are comprised of trees with low (0.26 to 0.45) and

medium form factor (0.51 to 0.61) respectively. Form factors for *S.birrea* were shown to decrease along the F1 axis, whilst those for *T.sericea*, *C.mopane*, *C.imberbe*, *D.cinerea* and *C.apiculatum* decreased along the F2 axis.

Table 3.10: The amount of information (eigenvalues) and variation (variability %) in form factor accounted for by each principal component

	F1	F2	F3	F4	F5	F6	F7
Eigenvalue	3.894	1.254	0.700	0.585	0.369	0.142	0.056
Variability (%)	55.622	17.913	9.995	8.355	5.278	2.030	0.807
Cumulative %	55.622	73.535	83.530	91.885	97.163	99.193	100.000

Table 3.11: Squared cosine values reflecting the representation quality of each variable along principal components F1 to F8. The figures in bold represent the highest squared cosine values for each variable

	F1	F2	F3	F4	F5	F6	F7
Form Factor	**0.438**	0.290	0.033	0.086	0.149	0.000	0.003
taper	**0.479**	0.109	0.095	0.223	0.092	0.001	0.001
form quotient	0.184	**0.478**	0.074	0.263	0.000	0.001	0.000
crown width	**0.823**	0.019	0.018	0.002	0.074	0.053	0.010
wd	0.339	0.200	**0.437**	0.010	0.005	0.005	0.003
diameter	**0.688**	0.157	0.032	0.000	0.049	0.074	0.000
height	**0.943**	0.001	0.010	0.000	0.000	0.007	0.039

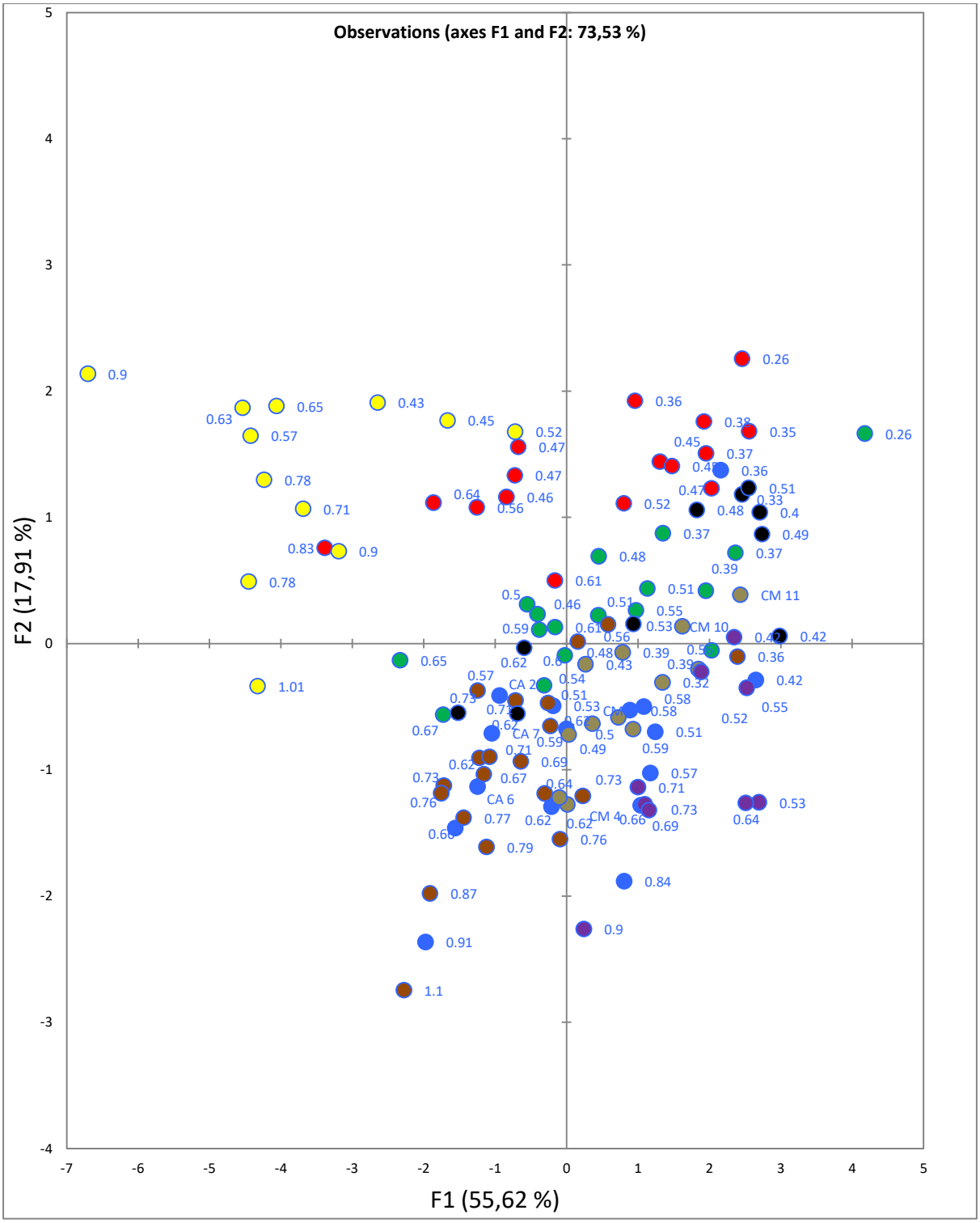

Figure 3.7: Ordination plot showing the distribution of form factors for individual trees of each species, with each colour representing a different species. The axis F1 and F2 are mainly related to tree height and form quotient, respectively. The colours for each species are as follows: *Terminalia sericea* (red), *Combretum apiculatum* (blue), *Sclerocarya birrea* (green), *Dichrostachys cinerea* (orange), *Lannea Schweinfurthi* (black), *Colophospermum mopane* (tan), *Combretum imberbe* (purple), *Portulacari afra* (yellow).

Chapter 4: Discussion

Comparisons of regression formulae derived from in situ and image measurements

Stem diameter and node length data required to construct a fractal model for tree volume, were collected using a manual in-field and a photographic approach. Results showed that measurements taken of images underestimated stem diameter and node length by 4% and 5% respectively, which are relatively small amounts. Under or over-estimation of stem diameter may be as a result of failure to clearly see the edges of the stem. Takahashi *et al*. (2007) state that the standard measurement error in stem diameter is 2% for images taken near tree and 5% for those taken further away and the error for this study is within the specified range. Other authors for example Shimizu *et al*. (2014) had errors in the range 2% to 4% for their sample trees. The error in height measurement for the study was smaller as compared to that of Takahashi *et al*. (2007) which was 10.25% and this might be attributed to the different tree sizes for each study. Height of sample trees ranged from 0.8m to 15.9m but only 4% of the trees were more than 10m, as compared to the Takahashi *et al*. (2007) sample in which the height ranged from 10m to 24m. Therefore the margin of error in height measurement from images is likely to be higher amongst taller trees than the shorter ones.

Since the stem diameter and height data from image and *in situ* measurements were not very different from each other, we would expect the fractal relationships developed using both datasets not to be statistically different. Statistical results showed that the interaction effects for the relationships between stem diameter and branch ratio, branch taper and node length, respectively; were not statistically significant, meaning that it does not matter which method is used for data collection, since for each species both the manual in-field and image analysis approach yield branch ratios, taper ratios and node lengths that are not statistically different from each other. The above statistical evidence coupled with the fact that errors in height and stem diameter measurements taken of images were within the standard acceptable errors, proves that data needed to construct a fractal model for tree volume can be collected in a sufficiently accurate way using dry season photographs.

A clear unobstructed view of the entire tree was a prerequisite in the selection of the sample trees but many of the trees had overlapping branches and were in close proximity to each other. This narrowed the selection range for the sample trees resulting in a small sample size ($n<20$) for each species. Even though there were many trees of each species at each study site, very few of them satisfied the requirement for a clear unobstructed view. This serious

limitation makes dry season photographs to be an inefficient way of collecting measurements required in fractal allometry. Though this form of remote data collection can be used in savannas where a small sample size can be selected, it is inapplicable to woodlands and natural forests were trees are densely populated.

Time taken to collect fractal allometry data using the photographic approach was twice the amount taken using the manual in-field approach. Measuring tree dimension parameters from images requires a number of steps and this lengthens the period for the method. The initial step involves climbing a tree so as to wrap coloured tape around its stem at each measurement point, followed by the capturing of the tree image. Thereafter the image is imported into IrfanView image processing software where stem diameters and node lengths are measured. Accurate measurements on images require one to magnify the tree image and the processing of the image further lengthens the time taken. The longer period taken to measure tree dimension parameter using images as compared to *in situ* measurements further contributes to the inefficiency of the former in collecting fractal allometry data.

The low coefficient of determination values of both the equations for the relationship between branch ratio and stem diameter derived from *in situ* and image measurements show the independence of branch ratio on stem diameter, thereby establishing the viability of the fractal allometry model and validating its assumptions

Model fitting and the comparisons between the new and existing empirical allometry

The usefulness of an allometric equation depends on the ability to quantify the error associated with the equation, and this can be done by deriving the confidence intervals of the estimates from the equation (Nickless *et al*., 2011). However a major constraint of the study was the unavailability of an independent stem-by-stem dataset, which made it impossible to provide biomass estimates from the new allometry, independent of the derived estimates based on equations fitted to all the stems from a species. This made it impossible to rigorously quantify the error associated with the new allometric equations. The existing empirical allometry is also uncertain. According to Netshiluvhi and Scholes (2001), the equations given in Table 3.5 are not fully defined as there is no information on the bias and variance of the fit, as well as the confidence intervals of the predicted values.

As a result, a comprehensive comparison of the new allometry against the existing empirical allometries to show which of the equations performed better could not be done, as only the confidence intervals of the slope and intercepts were compared. Colgan *et al*. (2013)

allometry had the narrowest confidence interval for the slope and intercept for each species (except *D.cinerea* which was not part of their study species), implying that it is the most precise allometry, which is not the same thing as most accurate (with the least bias). Arguably, for the assessment of plot biomass, where many stems are involved, accuracy is more essential than precision.

Fitting the model $M=bD^a$ provided no information on the value of including the form factor in biomass equations. It is possible to infer from the range of form factors derived here (0.43 to 0.69), and the non-unitary slopes of the regression of new allometry on the best empirical allometry by Colgan *et al*. (2013) (both in the form $\ln(M) = \beta_0^* + \beta_1^* \ln(F\rho D^2 H)$; that addition of from factors can improve fit by up to 11%. Therefore, the inclusion of species-specific form factor increases the precision of biomass estimation relative to equations not including a form factor. Other authors have tested the hypothesis and come to a similar conclusion. Including form factor in volume equations has been shown to improve the precision of volume estimation in plantation forestry (Adenkule *et al*., 2013) for example in Eucalyptus species (Gama *et al*., 2010). MacFarlene and Ver Planck (2012) showed that form factor explained a great proportion of the relative error in biomass estimation for hardwoods in Michigan. Including form factor in biomass equations reduces the error that arises from assuming that the tree stem is a perfect cylinder (Adenkule *et al*., 2013). Weiskittel *et al*. (2015) state that including additional variables for example form factor and wood density in allometric equations can improve their precision.

Form factor and its relationship with other tree attributes

Species-mean form factors estimated by the fractal allometry program were constantly lower as compared to those derived by Colgan *et al*., (2013). This might be as a result of the difference in tree sizes, as some of the researcher's sample trees had diameters and heights outside the ranges considered by Colgan *et al*. (2013).

Form factor was negatively correlated with wood density, basal stem diameter and height, meaning an increase in any of those variables corresponds with a decrease in form factor. The weak correlation between form factor and wood density means that the former cannot be estimated from the latter in future studies. Wood density was positively correlated with both basal diameter and height. This important, because wood density is also used in the new allometric form; therefore there is cross-correlation between two input variables which should in principle be independent of one another. Bruce and Max (1990) showed that form

factors changes with tree size. They argue that within a height class, form factors will decrease as diameter increase, and this is line with the results of this study. However they also state that form factor is positively correlated with height and this is contradicts the results of this study.

Estimation of form factors from easily observable tree traits

The distribution of form factors for *S.birrea* trees along the F1 axis implies that a form factor can be assigned to the species using height. Form factors for *S.birrea* were shown to decrease along the F1 principal component implying that for the species, tall trees are likely to have a smaller form factor as compared to the taller ones. This finding is consistent with the results shown in the correlation analysis which showed a negative correlation between form factor and height. However Bruce and Max (1990), argue that form factor is positively correlated with height meaning that the former decreases as the latter decreases.

The distribution of the form factors for *T.sericea, C.mopane, C.imberbe, D.cinerea* and *C.apiculatum* trees along the F2 axis suggests that the form factor for those species can be assigned using the form quotient. This means that after one has measured the basal stem diameter and the diameter just before the first branch and calculated the ratio of the two diameters, they can go on to assign a form factor to that tree. The decrease in form factor along the F2 axis confirms the negative correlation between form factor and stem diameter. This result is consistent with the argument by Bruce and Max (1990) who state that form factor decreases as stem diameter increases.

The F1 and F2 principal components which were chosen as the axis for the ordination plot to map trends for form factor were mainly related to tree height and form quotient, respectively. This means that the form factors of the study species can be assigned if data on tree height and form quotient is available. Tree height and the diameters needed to calculate the form quotient can be measured with sufficient accuracy from photographs of trees as shown in the second paragraph of this chapter. This means that form factors of South African trees can be assigned using few simple measurements of height and stem diameters taken from photographs.

However the assigning of a form factor to tree by a visual assessment a photograph of the tree was inapplicable for this study as this approach required the distance between the photographer and each sample tree to be the same throughout data collection. The requirement for a clear unobstructed view for each sample tree meant that the researcher had

to select the ideal horizontal distance from their focal point to the object (tree), which would allow a clear view of the tree before its capture. Some of the trees were obstructed either by whole trees or overlapping branches, thus the distance from which the image was captured was dependent on whether or not the researcher could get a clear shot of the whole tree. Sample trees were of different sizes, meaning that the bigger the tree the further away the researcher had to stand in order to take a picture of the whole tree, and vice versa. These challenges resulted in great variation in the horizontal distances between the focal point and each sample tree.

Chapter 5: Conclusion

This study proves that the error in measuring tree dimension parameters using dry season photography is well within the acceptable range of dendrometric measurements. Thus deriving vital tree measurements from photographs is sufficiently accurate for the purposes of biomass and volume estimation. Less time is spent in the field capturing the image of each sample tree as compared to measuring tree dimension parameters *in situ*, and this can result in significant cost savings and a faster way of collecting field data. However the time it takes to collect measurements using images is lengthened during the processing of the images to allow measurements in IrfanView, resulting in a longer period for image measurements when compared to the *in situ* ones. Fractal allometry relationships derived using both methods were not statistically significant, and this means that tree volume can be modelled using a dataset from *in situ* or image measurements.

South African trees can be assigned a form factor, with an accounted variance of about 73.5%, using easy field measurements of tree height and form quotient. Principal Component Analysis showed that the variation in form factor was mainly explained by these two variables. It is hard to accurately collect tree height data *in situ*, and that is where photographic approach comes in. This method of assigning form factors to South African trees saves us the trouble of having to cut down trees, weigh them and measure their cylindrical mass so as to calculate the form factor.

The other suggested method of assigning a form factor to a tree by simply looking at its photograph may work if the image of each sample tree is captured at about the same horizontal distance away from the tree. This is rarely possible as the trees are often of different sizes and may be obstructed by other sample trees or overlapping branches.

The study could not determine whether including a species-specific form factor would result in new allometry that performs better that the existing empirical allometry, as there was no independent data set to quantify the error associated with the former, but by logical inference, an allometry which includes form factor information could be both more precise and accurate than one that does not. Furthermore, the speed and ease with which data can be collected, and the removal of the need to fell, dry and weigh the sample trees, makes the combination of a fractal allometry volume estimation and a derived form factor very attractive for assigning allometric equations to large number of African species for which they are unknown

References

Adekunle, V. a.J., Nair, K.N., Srivastava, A.K., Singh, N.K., 2013. Models and form factors for stand volume estimation in natural forest ecosystems: a case study of Katarniaghat Wildlife Sanctuary (KGWS), Bahraich District, India. Journal of Forestry Research, 24, 217–226.

Arastu, R., 1998. Leonardo was wise: trees conserve cross-sectional area despite vessel structure. Journal of Young Investigators, 1, 1–20.

Armer, G., 2002. Monitoring and Assessment of Structures. CRC Press.

Barrett, A., Brown, L., 2012. A novel method for estimating tree dimensions and calculating canopy volume using digital photography. African Journal of Range and Forage Science, 29, 153–156.

Blozan, W., 2006. Tree measuring guidelines of the eastern native tree society. Bulletin of the Eastern Native Tree Society, 1, 3–10.

Bombelli, A., Avitabile, V., BelelliMarchesini, L., Balzter, H., Bernoux, M., Hall, R., Henry, M., *et al*., 2009. Assessment of the status of the development of the standards for the terrestrial essential climate variables: biomass. Food and Agriculture Organization.Global Terrestrial Observation System. Rome.

Breidenbach, J., Antón-Fernández, C., Petersson, H., McRoberts, R.E., Astrup, R., 2014. Quantifying the model-related variability of biomass stock and change estimates in the Norwegian National Forest Inventory. Forest Science, 60, 25–33.

Bruce, D., Max, T.A., 1990. Use of profile equations in Tree volume estimation.

Burkhart, H.E., Tomé, M., 2012. Modeling Forest Trees and Stands. Springer Science & Business Media.

Cannell, M.G.R., 1984. Woody biomass of forest stands. Forest Ecology and Management, 8, 299–312.

Carsan, S., Orwa, C., Harwood, C., Kindt, R., Stroebel, A., Neufeldt, H., Jamnadass, R., 2012. African Wood Density Database.World Agroforestry Centre, Nairobi

Clark, N.A., Wynne, R.H., Schmoldt, D.L., Winn, M., 2000. An assessment of the utility of a non-metric digital camera for measuring standing trees. Computers and Electron in Agriculture, 28, 151–169.

Colgan, M.S., 2012. Tree Biomass in South African Savannas: Flying over, hugging and destroying tree to save them. Doctor of Philosophy Dissertation, Stanford University, Carlifonia, United States of America

Colgan, M.S., Swemmer, T., Asner, G.P., 2013. Structural relationships between form factor, wood density, and biomass in African saVan na woodlands. Trees 28, 91–102.

Chave, J., Andalo, C., Brown, S., Cairns, M.A., Chambers, J.Q., Eamus, D., *et al.*, 2005. Tree allometry and improved estimation of carbon stocks and balance in tropical forests. Oecologia 145, 87–99.

Chave, J., Réjou-Méchain, M., Búrquez, A., Chidumayo, E., Colgan, M.S., Delitti, W.B.C., *et al*., 2014. Improved allometric models to estimate the aboveground biomass of tropical trees. Global Change Biology, 20, 3177–3190.

Da Silva, F., Suwa, R., Kajimoto, T., Ishizuka, M., Higuchi, N., Kunert, N., 2015. Allometric equations for estimating biomass of Euterpe precatoria, the most abundant palm species in the Amazon. Forests 6, 450–463.

Gayon, J., 2000. History of the Concept of Allometry 1. American Zoologists, 40, 748–758.

Gevorkiantz, S.R., Olsen, L.P., 1955. Composite volume tables for timber and their application in the Lake States. US Department of Agriculture.

Gray, H.R., 1956. The form and taper of forest-tree stems. Imperial Forestry Institute, University of Oxford.

Gray, H.R., 1966. Principles of forest tree and crop volume growth: a mensuration monograph. Australian Bulletin of Forestry and Timber Bureau. 42

Goodman, P.S., 1990. Soil, vegetation and large herbivore relations in Mkuzi Game Reserve, Natal. PhD Thesis, University of the Witwatersrand, Johannesburg, South Africa

Henry, M., Jara, M.C., Réjou-Méchain, M., Piotto, D., Fuentes, J.M.M., Wayson, C., Guier, F.A., Lombis, H.C., López, E.C., Lara, R.C., others. 2015. Recommendations for the use of tree models to estimate national forest biomass and assess their uncertainty. Annals of Forestry Science, 72, 769–777.

IPCC 2000. Summary for Policy makers: Emissions Scenarios. A Special Report of Working Group III of the Intergovernmental Panel on Climate Change.

Jordan, L., Berenhaut, K., Souter, R., Daniels, R.F., 2005. Parsimonious and completely compatible taper, total, and merchantable volume models. Forest Science, 51, 578–584

Kamatou, G.P., 2003. The allometry of four savanna tree species determined by fractal methods. MSc thesis, University of the Witwatersrand, Johannesburg, South Africa.

Ketterings, Q.M., Coe, R., Van Noordwijk, M., Ambagau, Y., Palm, C.A., 2001 Reducing uncertainty in the use of allometric biomass equations forpredicting above-ground tree

biomass in mixed secondary forests. Forest Ecology and Management, 146(1-3): 199-209

Komiyama, A., Poungparn, S., Kato, S., 2005. Common allometric equations for estimating the tree weight of mangroves. Journal of Tropical Ecology, 21, 471–477.

Konôpka, B., Pajtík, J., Šebeň, V., Lukac, M., 2011. Belowground biomass functions and expansion factors in high elevation Norway spruce. Forestry, 84, 41–48.

Kuyah, S., Dietz, J., Muthuri, C., Jamnadass, R., Mwangi, P., Coe, R., Neufeldt, H., 2012. Allometric equations for estimating biomass in agricultural landscapes: I. Aboveground biomass. Agriclture, Ecosystems and Environment, 158, 216–224.

Le Quéré, C., Andrew, R.M., Canadell, J.G., Sitch, S., Korsbakken, J.I., Peters, G.P. *et al*., 2016. Global carbon budget 2016. Earth System Science Data, 8, 605.

Lu, D., 2006. The potential and challenge of remote sensing-based biomass estimation. International Journal of Remote Sensing, 27, 1297–1328.

Martin, F.S., Navarro-Cerrillo, R.M., Mulia, R., Van Noordwijk, M., 2010. Allometric equations based on a fractal branching model for estimating aboveground biomass of four native tree species in the Philippines. Agroforestry Systems, 78, 193–202.

MacFarlane, D.W., Kuyah, S., Mulia, R., Dietz, J., Muthuri, C., Van Noordwijk, M., 2014. Evaluating a non-destructive method for calibrating tree biomass equations derived from tree branching architecture. Trees 28, 807–817.

MacFarlene, D.W., Ver Planck, N.R., 2012. Improved predicition of hardwood tree biomass derived from wood density estimates and form factors for whole trees. Northen Research Station - US Forest Service.

Martin, F.S., Navarro-Cerrillo, R.M., Mulia, R., Van Noordwijk, M., 2010. Allometric equations based on a fractal branching model for estimating aboveground biomass of four native tree species in the Philippines. Agroforestry Systems, 78, 193–202.

Munnik, M.C., Verster, E., Rooyen, T.H.V., 1996. Spatial pattern and variability of soil and hillslope properties in a granitic landscape. 3. Phalaborwa area. South African Journal of Plant and Soil, 13, 9–16.

Návar, J., 2010. Measurement and assessment methods of forest aboveground biomass: a literature review and the challenges ahead. Biomass InTech Rij. Croatia. 27–64.

Netshiluvhi, T.R., Scholes, R.J., 2001. Allometry of South African woodland trees. Report ENV-P-1 2001-007, CSIR, Pretoria

Newnham, R.M., 1965. Stem form and the variation of taper with age and thinning regime. Forestry 38, 218–224.

Newnham, R.M., 1956. A study of form and taper of stems, of Douglas fir, western hemlock, and western red cedar on the University Research Forest, Haney, British Columbia. University of British Columbia.

Nickless, A., Scholes, R.J., Archibald, S., 2011. A method for calculating the variance and confidence intervals for tree biomass estimates obtained from allometric equations. South African Journal of Science, 107, 86–95.

Picard, N., Saint-Andre, L., Henry, M., 2012. Manual for building tree volume and biomass allometric equations: from field measurement to prediction. FAO/CIRAD.

Pelletier, G., Landry, D and Girouard, M., 2013. A tree classification system for New Brunswick. Northern Hardwoods Research Institute. Edmundstown, New Brunswick.

Picard, N., Saint-Andre, L., Henry, M., 2012. Manual for building tree volume and biomass allometric equations: from field measurement to prediction. FAO/CIRAD.

Rosette, J.A.B., North, P.R.J., Suarez, J.C., Los, S.O., 2010. Uncertainty within satellite LiDAR estimations of vegetation and topography. International Journal of Remote Sensing, 31, 1325–1342.

Sala, N., 2013. Fractal geometry and Superformula to model natural shapes

Samalca, I.K., 2007. Estimation of Forest Biomass and its Error: A case in Kalimantan. Indones. MSc, University of Southampton, United Kingdom.

Schenk, T., 2005. Introduction to photogrammetry. Ohio State University, Columbus, USA.

Scholes, R.J., 1988. Response of three semi-arid savannas on contrasting soils to the removal of the woody component. PhD Thesis, University of the Witwatersrand, Johannesburg, South Africa.

Shackleton, C.M., 1997. The prediction of woody productivity in the savanna biome, South Africa. PhD Thesis, University of the Witwatersrand, Johannesburg, South Africa

Shackleton, C.M., 2001. Managing regrowth of an indigenous savanna tree species (*Terminalia sericea*) for fuelwood: the influence of stump dimensions and post harvest coppice pruning. Biomass and Bioenergy, 20, 261-267

Shelbourne, C., Namkoong, G., 1966. Photogrammetric technique for measuring bole straightness. Presented at the Proceedings of the eight southern conference on forest tree improvement, June, pp. 16–17.

Shettles, M., Temesgen, H., Gray, A.N., Hilker, T., 2015. Comparison of uncertainty in per unit area estimates of aboveground biomass for two selected model sets. Forest Ecology and Management. 354, 18–25.

Shimizu, A., Yamada, S., Arita, Y., 2014. Diameter Measurements of the Upper Parts of Trees Using an Ultra-Telephoto Digital Photography System. Open Journal of Forestry, 4, 316.

Socha, J., Kulej, M., 2007. Variation of the tree form factor and taper in European larch of Polish provenances tested under conditions of the Beskid Sądecki mountain range (southern Poland). Journal of Science, 53, 538–547.

Takahashi, M., Saito, K., Shiraishi, N., Iehara, T., Takahashi, F., 1997. A photo based measurement system using a measuring camera. Journal of Forest Planning 3, 1–9.

Tietema, T., (1993). Biomass determination of fuelwood trees and bushes of Botswana, Southern Africa. Forest Ecology and Management, 60, 257-266.

Van Noordwijk, M., Mulia, R., 2002. Functional branch analysis as tool for fractal scaling above-and belowground trees for their additive and non-additive properties. Journal of Ecological Modelling, 149, 41–51.

Van Noordwijk, M., Spek, L.Y., de Willigen, P., 1994. Proximal root diameter as predictor of total root size for fractal branching models. Journal of Plant and Soil, 164, 107–117.

Van Vuuren, N.J.J, Banks, C.H., StoHR, H.P., 1978. Shrinkage and Densities of timbers used in Republic of South Africa. Bulletin 57. Department of Forestry, Pretoria

Van Wyk, P., 1972. Tree of the Kruger National Park. 2 volumes. Purnell, Cape Town, South Africa.

Ver Planck, N.R., MacFarlane, D.W., 2014. Modelling vertical allocation of tree stem and branch volume for hardwoods. Forestry, 87, 459–469.

Washusen, R., 2002. Tension wood occurrence in Eucalyptus globulus Labill. II. The spatial distribution of tension wood and its association with stem form. Journal of Australian Forestry, 65, 127–134.

Weiskittel, A.R, MacFarlene, D.W, Radtke, P.J, Affleck, D.L.R, Temesgen, H, Woodall, C.W, Westfall, J.A., Coulston, J.W., 2015. A call to improve methods for estimating tree biomass for regional and national assessments. Journal of Forestry, 113 (4): 414-424

West, P.W., 2009. Tree and Forest Measurement. 2nd Edition. Springer Dordrecht Heidelberg London New York, USA.

Zhang, D., Samal, A., Brandle, J.R., 2007. A method for estimating fractal dimension of tree crowns from digital images. International Journal of Pattern Recognition and Artificial Intelligence, 21, 561–572.

Appendix 1: The fractal allometry programme

```
Fractal allometry programme (Courier font 10).
PROGRAMME FractalGu;

{-------------------------------------------------------------------}

Uses fractal properties to estimate the wood mass, twig mass,
bark mass, whole tree (aboveground) mass and stem area
of trees. Version developed for use by T. Muzite
R.J Scholes, Environmentek, CSIR
November 2015

{-------------------------------------------------------------------}

uses wincrt;
const heap size=1000; {number of recursive nodes that can be recalled}
type equation type= (none, linear, quadratic, loge, InIn, log10, loglog,
power, exponent, unknown);
const formlist: array [equationtype] of string [4] =
                ('none', 'line', 'quad', 'loge', 'InIn', 'lg10', 'lglg',
'powr', 'expt', 'unkn');
      var diam: array [1..heapsize] of real; {heap of cross-sectional
areas}
      Ta, Tb, La, Lb, Wa, Wb, Ba, Bb, Va, Vb, Asd,
      WoodDensity, Barkdensity, TermTwigd,
      sumWoodMass, SumTwigMass, SumBarkMass, Sumwoodvol, SumBarkVol
,BranchVol
      ccm, woodvol, barkvol, bolevol, twigmass, woodmass, rcm, rm, Am²
      In10, Nodelength, acm², dmm, dcm, dm, barkthick, woodarea,
      dterm, stemArea, SumStemArea, assym, c², Area of Branches: real;
      n,1,decile, ntwigs: integer;
      par: text;
      bole form, bark form, twig form, taperform, node form:equation type;
      form name: string  [4];
      species code: string [8];
      response , sp : char
d     descriptor:string [30];
A     AS:array [0..10] of real;

{-------------------------------------------------------------------}
```

```
Function BranchAssymetry: real;
{the asymmetry of branching is expresses as the

(area of branch 1)/ (area of branch 1 + 2)

It therefore is constrained to between 0 and 1, with a mean of 0,5 and is
assumed
to be normally distributed.
The normal distribution is described by the standard deviation of the
asymmetry}
var randnum,bigger,z:real;                                          Function
InvNormal (var q:real) :real;
{given the probability of x>z, determines value of z }
var x, sqrtx, cubex: real;
begin
      x: = sqrt (In (1.0/sqr (q)));
      sqrx: sqrt (x);
      cubex : = sqrtx*x;
      InvNormal : = x- ((2.515517+0.802853*0.010328*sqrtx)/
            (1.0+1,432788*x+0.189269*0.00138*cubex));
      end;
begin
      {Generate a random  number between 0.5 and 1.0}
      randomize;
      randnum: = 0.5+random (20000)/40000.0;
      z: = InvNormal (randnum);
      bigger: = z*Asd+0.5;
      if bigger>1.0 then BranchAssymetry:=1.0 else BranchAssymetry: =
bigger;
end;
{-------------------------------------------------------------------------}
function Solve (var x, a, b:real; var eqt:equation type) : real;
begin
{Solve the equation}
if x>0.000000001
      then
      case eqt of
            linear      : solve: = a*x+b;
            quadratic   : solve: = (a*sqr (x)) +b;
            loge  : solve: = a*In (x)+b ;
            InIn  : solve: = exp (a*In (x)+b);
```

```
            log10 : solve:= a*In (x)/In10+b;
            loglog      : solve:= exp ((a*In (x)/In10+b)*In10);
            power : solve := (exp (a*In (x)))*b;
            exponent    : solve := exp (b*In (x))*a;
            end {of case}
      else Solve : = 0.0;
end; { of equationbuilder}
{-------------------------------------------------------------------------}
Procedure Branch;
var area,sum area:real;
begin
end;
{Main programme }
{-------------------------------------------------------------------------}
Begin
In10: = In (10.0);
{define database file}
write ('Species code? (4letter genus+4letter species)>'); readIn
(species Code);
assign (par, 'a:\'+species code +'.par');
reset (par);
{read in database file}
{header lines first}
for 1:=1 to 2 do readIn (par); {header lines}
{now the data, write them out as a check}
readIn (par, descriptior, woodDensity);
writeIn (descriptor, WoodDensity: 8:3);
readIn (par, descriptor, BarkDensity);
writeIn (descriptor, BarkDensity: 8:3);
readIn (par, descriptor, TermTwigd);
writeIn (descriptor, TermTwigd:8:3);
TermTwigD: = termTwigD/10.0;
{bole volume}
readIn (par, descriptor, formname:Va,Vb);
writeIn (descriptor:30,formname:4,Va:8:3,Vb:8:3);
boleform: = none;
repeat

bole form: = succ (bole form)
until (formname = form list[bole form]) or (bole form = unknown);
{bark thickness}
```

```
readIn (par, descriptor, form name, Ba,Bb);
writeIn (descriptor:30, form name:4, Ba:8:3, Bb:8:3);
bark form: = none;
repeat
barkform: = succ (bark form)
until (formname = formlist [bark form]) or (bark form = unknown);
{twigmass}
readIn (par, descriptor: form name, Wa, Wb);
writeIn (descriptor:30, form name:4,Wa:8:3, Wb:8:3);
twigform: = none;
repeat
twigform: = succ (twig form)
until (form name=form list [twig form]) or (twig form = unknown);
{taper}
readIn (par, descriptor, form name, Ta, Tb);
writeIn (descriptor:30, form name:4, Ta:8:3, Tb:8:3);
taper form: none;
repeat
taper form: = succ (taper form)
until (formname = formlist [taper form]) or (taper form = unknown);
{node length}
readIn (par, descriptor, form name, La, Lb);
writeIn (descriptor:30, form name:4, La:8:3, Lb:8:3);
node form: = none;
repeat
node form: = succ (node form)
until (form name = form list [node form]) or (node form = unknown);
{asymmetry}
readIn (par, descriptor, ASD);
WriteIn (descriptor:30,ASD:8:4);
Close (par);
      Write ('Input parameters read in. Press any key to continue…');
readIn;
repeat            { continue until user quits}

            {Set accumulators to zero}
            SumTwigMass: = 0.0;
            SumWoodVol: = 0.0;
            SumBarkVol; = 0.0;
            SumStemArea; = 0.0;
            ntwigs: = 0;
```

```
      {obtain the basal diameter}
      write('What is the basal circumference? (cm)> ');
      readIn (ccm); WriteIn;
      dcm: ccm/pi; {diameter, cm}
      dm: dcm/100.0; {diameter in metres}
      acm²: = pi*sqr(dcm*0.5); {XS area, cm²}
            clrscr;
      WriteIn('Circumference = ',ccm:6:1,'cm; Diameter = 'dcm:6:1,'
      cm; Area = ',acm2:6:0, ' cm²');
      {Calculate the volume of the main bole, in m3}
            bolevol: = Solve (dm,Va,Vb,boleform); {outside bark bole
      volume, m3}
      if bolevol <0.0 then bolevol: =0.0;
      {stem surface area}
      StemArea: = (dcm*pi/100.0)*(bolevol/(acm2/10000.0));
      SumStemArea: SumStemArea+StemArea;
      {the bark volume on the main bole}
      BarkThick: = Solve(dcm,Ba,Bb,bark form)/10.0; {cm)
      if BarkThick<0.0 then BarkThick:0.0;
      if BarkThick >=rcm then bark thick:=rcm;
      BarkVol: = StemArea*barkthick/100.0; {m³}
      SumBarkVol: = SumBarkVol+BarkVol;
      Woodvol:=Bolevol-barkVol;
      if Woodvol <0.0 then Woodvol: = 0.0; {m³}
      SumWoodVol: = SumWoodVol+WoodVol;
      BoleVol: = Bolevol-BarkVol;
      {Calculate the area of the first 2 branches}
      assym: = 0.5;
      c²  := ccm*ccm;
      Area of Branches: = (Solve (c²,Ta,Tb,taper from)*c²)/(4.0*pi);
      {sum of XS area above branch}

if Area of Branches<0.0 then Area of Branches:=c²/(4.0*pi);
diam[1]:=sqrt (4.0*(Area of Branches*Assym)/pi);
diam[2]:=sqrt (4.0*(Area of Branches*(1.0-Assym))/pi);
n: = 2;
{commence the fractal recursion}
repeat
      if diam[n] > termTwigD
            then {work out stem volume and carry on branching}
            begin
```

```
            dcm: = diam[n];
            acm²: = pi*sqr(dcm/2.0);
            Node Length: = Solve (dcm,La,Lb,node form); {in cm}
            if node length < 0.0 then node length: = 1.0;
                  BranchVol: = Node length*acm²/1000000.0; {m3}
            StemArea: = (dcm*pi/100.0)*(branchvol/(acm2/10000.0));
            SumStemArea: = SumStemArea+StemArea;
            BarkThick: = Solve (dcm,Ba,Bb,bark form);
                  if Bark Thick < 0.0 then Bark Thick: 0.0;
            if (2.0*BarkThick) > dcm then barkthick: = dcm*0.5;
            Barkvol: = (BarkThick/1000.0)*StemArea;
            SumBarkVol: = SumBarkVol+BarkVol;
            Woodvol: = BranchVol-BarkVol;
            if WoodVol < 0.0 then WoodVol: = 0.0;
            SumWoodVol: = SumWoodVol+WoodVol;
            StemArea: = dcm*Nodelength/10000.0;
            assy: = 0.5;
                  c²: = sqrt (dcm*pi);
            Area of Branches: = (Solve (c²,Ta,Tb, taper
form)*c2)/(4.0*pi); {sum of XS area above branch};
            if Area of Branches < 0.0 then Area of Branches: =
c²/(4.0*pi);
            diam[n]: = sqrt (4.0*Area of Branches*Assym/pi);
            diam(n+1): = sqrt (4.0*Area of Branches*(1.0-Aassym)/pi);
            n: = n+1;
            end
      else {work out twig mass, and go back a branch}
            begin

            ntwigs: = ntwigs+1;
            dmm; = diam[n]*10.0;
         TwigMass: = Solve (dmm,Wa,Wb,twig form);
         if TwigMass < 0.0 then Twig mass:=0.0;
         SumTwig Mass: = SumTwig Mass+Twig Mass/1000.0;
            n:=n-1;
            end;
   until n = 0;
   SumWoodMass:=SumWoodVol*WoodDensity;
   SumBarkMass:=SumBarkVol*BarkDensity;
   WriteIn ('Fractal Allometry');
   WriteIn ('Twig Mass = ',SumTwigmass:8:1,' kg; Number of twigs
```

```
=',ntwigs:7,' smaller than ',TermTwigD:4:1,' cm');
   WriteIn ('Bark Mass= ',SumBarkMass:8:1,' kg; Bark
volume=', SumBarkVol:8:3,' m³);
   WriteIn ('Wood Mass= ',SumWoodMass:8:1,' kg; Wood volume =
',SumWoodVol:8:3,' m³; Main Bole = ',Bolevol:8:3,' m³');
  WriteIn ('Tree Mass = ',(SumWoodMass+SumBarkMass+SumTwigMass):8:1,'
kg');
  WriteIn ('Stem Surface Area = ',StemArea:8:4,' m2 Projected stem
area = ',StemArea/pi*0.5:8:4,' m²');
  writeIn;
  write ('Enter any key to continue, or <q>uit > ');
  readIn (response);
  until response = 'q';
  End
```

Appendix 2: An example of an input file for the FractalGu programme, showing the input parameters for *T.sericea*.

Parameters for Fractal allometry of *Terminalia sericea*

T Muzite March 2016

Wood density (kg/L)	: 0.749
BarkDensity (kg/L)	: 0.39
Terminal Twig diameter (mm)	: 10.0
Assymetry (Al/(Al+As)	: 0.5
Bark thickness (cm) = Ba*ln(dcm)+Bb	: 0.2295 0.2693
Twigmass (g) = Wa*twigdiam(mm)+Wb	: 2.0 0.0
Branch taper (%/cm) = Ta*dcm+Tb	: 0.0 0.369
Node length (cm) = La*ln(dcm)+Lb	: 1.3585 77.469
Area above:area below=Aa*Topdcm+Ab	: 0.0 1.2027

Appendix 3.1: Summary of regression formulae for the relationship between branch ratio (unit less) and stem diameter (cm).

spp	method	Coeff		SE	T	p	Upper CI	Lower CI	R^2	n
TS	1	β_0	1.203	0.049	24.672	0.000	1.105	1.301	0.000	53
		β_1	0.000	0.003	0.138	0.891	-0.005	0.006		
TS	2	β_0	1.201	0.041	29.104	0.000	1.118	1.284	0.001	53
		β_1	0.000	0.002	0.194	0.847	-0.004	0.005		
CA	1	β_0	1.197	0.047	25.250	0.000	1.102	1.292	0.000	51
		β_1	1.232E-5	0.005	0.002	0.998	-0.010	0.010		
CA	2	β_0	1.194	0.045	26.812	0.000	1.105	1.284	0.000	51
		β_1	5.200E-5	0.005	0.011	0.992	-0.010	0.010		
SB	1	β_0	1.124	0.041	27.618	0.000	1.042	1.206	0.026	53
		β_1	0.002	0.002	1.196	0.237	-0.001	0.006		
SB	2	β_0	1.124	0.035	32.121	0.000	1.054	1.194	0.022	53
		β_1	0.002	0.002	1.086	0.282	-0.001	0.005		
DC	1	β_0	1.286	0.038	33.718	0.000	1.210	1.362	0.020	59
		β_1	-0.005	0.005	-1.073	0.288	-0.016	0.005		
DC	2	β_0	1.314	0.039	33.545	0.000	1.236	1.392	0.077	59
		β_1	-0.012	0.006	-2.184	0.033	-0.023	-0.001		

Appendix 3.1: continued

spp	method	Coeff		SE	T	p	Upper CI	Lower CI	R^2	n
LS	1	β_0	1.157	0.061	18.880	0.000	1.032	1.282	0.016	33
		β_1	0.001	0.002	0.712	0.482	-0.002	0.005		
LS	2	β_0	1.257	0.053	23.754	0.000	1.149	1.365	0.042	33
		β_1	-0.002	0.002	-1.163	0.254	-0.005	0.001		
CM	1	β_0	1.226	0.047	26.354	0.000	1.132	1.319	0.001	47
		β_1	0.000	0.003	-0.185	0.854	-0.007	0.006		
CM	2	β_0	1.205	0.048	25.264	0.000	1.109	1.301	0.000	47
		β_1	0.000	0.003	0.050	0.960	-0.007	0.007		
CI	1	β_0	1.295	0.063	20.722	0.000	1.168	1.422	0.129	37
		β_1	-0.008	0.004	-2.274	0.029	-0.015	0.000		
CI	2	β_0	1.315	0.061	21.448	0.000	1.190	1.439	0.168	37
		β_1	-0.009	0.003	-2.655	0.012	-0.016	-0.002		
PA	1	β_0	1.164	0.060	19.446	0.000	1.043	1.285	0.029	41
		β_1	-0.008	0.008	-1.079	0.287	-0.024	0.007		
PA	2	β_0	1.187	0.057	20.919	0.000	1.072	1.302	0.077	41
		β_1	-0.014	0.008	-1.803	0.079	-0.030	0.002		

The equation is in the form $Br= \beta_{0+} \beta_1 D$ (where Br is branch ratio, β_0 and β_1 are regression coefficients, and D stem diameter. Method 1 is the *in situ* approach, while method 2 is the photographic approach

Appendix 3.2: Summary of regression formulae for the relationship between branch taper and stem diameter (cm).

spp	method	coeff		SE	T	p	Upper CI	Lower CI	R^2	n
TS	1	β_0	0.369	0.057	6.515	0.000	0.255	0.483	0.182	53
		β_1	-0.009	0.003	-3.334	0.002	-0.015	-0.004		
TS	2	β_0	0.301	0.046	6.586	0.000	0.209	0.393	0.127	53
		β_1	-0.006	0.002	-2.722	0.009	-0.011	-0.002		
CA	1	β_0	0.429	0.072	5.924	0.000	0.283	0.575	0.198	51
		β_1	-0.024	0.007	-3.440	0.001	-0.038	-0.010		
CA	2	β_0	0.293	0.034	8.590	0.000	0.224	0.361	0.246	51
		β_1	-0.013	0.003	-3.918	0.000	-0.020	-0.006		
SB	1	β_0	0.295	0.038	7.797	0.000	0.219	0.372	0.153	53
		β_1	-0.005	0.002	-3.005	0.004	-0.008	-0.002		
SB	2	β_0	0.288	0.037	7.854	0.000	0.215	0.362	0.155	53
		β_1	-0.005	0.002	-3.055	0.004	-0.008	-0.002		
DC	1	β_0	0.175	0.037	4.737	0.000	0.101	0.249	0.007	59
		β_1	0.003	0.005	.638	0.526	-0.006	0.012		
DC	2	β_0	0.198	0.042	4.675	0.000	0.113	0.284	0.003	59
		β_1	-0.002	0.005	-.413	0.681	-0.013	0.009		

Appendix 3.2: continued.

spp	method	coeff		SE	T	p	Upper CI	Lower CI	R^2	n
LS	1	β_0	0.157	0.031	5.051	0.000	0.094	0.221	0.058	33
		β_1	-0.001	0.001	-1.363	0.183	-0.003	0.001		
LS	2	β_0	0.173	0.039	4.389	0.000	0.092	0.253	0.029	33
		β_1	-0.001	0.001	-0.955	0.347	-0.003	0.001		
CM	1	β_0	0.308	0.067	4.590	0.000	0.173	0.444	0.072	47
		β_1	-0.008	0.004	-1.847	0.072	-0.017	0.001		
CM	2	β_0	0.261	0.057	4.551	0.000	0.145	0.376	0.044	47
		β_1	-0.005	0.004	-1.439	0.157	-0.013	0.002		
CI	1	β_0	0.181	0.045	4.047	0.000	0.090	0.271	0.027	37
		β_1	-0.002	0.002	-0.963	0.343	-0.007	0.003		
CI	2	β_0	0.214	0.043	4.987	0.000	0.127	0.301	0.096	37
		β_1	-0.004	0.002	-1.870	0.070	-0.009	0.000		
PA	1	β_0	0.632	0.094	6.704	0.000	0.441	0.823	0.205	41
		β_1	-0.037	0.012	-3.093	0.004	-0.061	-0.013		
PA	2	β_0	0.727	0.141	5.143	0.000	0.441	1.013	0.116	41
		β_1	-0.041	0.018	-2.263	0.029	-0.079	-0.004		

The equation is in the form $Bt = \beta_{0+} \beta_1 D$ (where Bt is branch taper, β_0 and β_1 are regression coefficients, and D stem diameter. Method 1 is the *in situ* approach, while method 2 is the photographic approach

Appendix 3.3: Summary of regression formulae for the relationship between internode length (cm) and stem diameter (cm).

spp	method	coeff		SE	T	p	Upper CI	Lower CI	R^2	n
TS	1	β_0	77.460	32.883	2.356	0.022	11.454	143.484	0.000	53
		β_1	1.359	11.852	0.115	0.909	-22.435	25.152		
TS	2	β_0	56.279	27.980	2.011	0.049	0.132	112.426	0.012	53
		β_1	8.138	10.289	0.791	0.433	-12.508	28.784		
CA	1	β_0	-30.899	31.897	-0.969	0.337	-95.000	33.201	0.214	51
		β_1	53.169	14.575	3.648	0.001	23.881	82.458		
CA	2	β_0	-19.752	33.192	-0.595	0.555	-86.454	46.950	0.179	51
		β_1	50.284	15.380	3.269	0.002	19.377	81.190		
SB	1	β_0	-24.866	50.985	-0.803	0.426	-87.014	37.281	0.223	53
		β_1	43.358	11.128	3.896	0.000	21.038	65.679		
SB	2	β_0	-26.189	31.292	-0.837	0.407	-89.011	36.633	0.220	53
		β_1	42.436	11.199	3.789	0.000	19.953	64.918		
DC	1	β_0	53.928	13.266	4.065	0.000	27.363	80.494	0.001	59
		β_1	-1.531	6.946	-0.220	0.826	-15.440	12.378		
DC	2	β_0	47.032	13.852	3.395	0.001	19.293	74.771	0.001	59
		β_1	1.271	7.367	0.173	0.864	-13.481	16.023		

Appendix 3.3: continued.

spp	method	coeff		SE	T	p	Upper CI	Lower CI	R^2	N
LS	1	β_0	53.851	31.139	1.729	0.094	-9.658	117.359	0.026	33
		β_1	8.756	9.575	0.914	0.368	-10.773	28.284		
LS	2	β_0	49.892	30.600	1.630	0.113	-12.516	112.301	0.031	33
		β_1	9.449	9.544	0.990	0.330	-10.016	28.914		
CM	1	β_0	26.541	37.685	0.704	0.485	-49.360	102.442	0.040	47
		β_1	19.955	14.629	1.364	0.179	-9.510	49.419		
CM	2	β_0	25.520	35.743	0.714	0.479	-46.470	97.511	0.042	47
		β_1	19.661	13.988	1.406	0.167	-8.512	47.834		
CI	1	β_0	-17.641	57.530	-0.307	0.761	-134.433	99.151	0.079	37
		β_1	35.917	20.704	1.735	0.092	-6.114	77.949		
CI	2	β_0	-25.954	56.004	-0.463	0.646	-139.648	87.741	0.094	37
		β_1	38.752	20.317	1.907	0.065	-2.494	79.998		
PA	1	β_0	2.576	11.891	0.217	0.830	-21.476	26.628	0.097	41
		β_1	12.235	5.987	2.043	0.048	0.124	24.345		
PA	2	β_0	2.311	9.240	0.250	0.804	-16.379	21.001	0.129	41
		β_1	11.734	4.888	2.400	0.021	1.846	21.622		

The equation is in the form $L= \beta_{0+} \beta_1 D$ (where L is node length, β_0 and β_1 are regression coefficients, and D stem diameter at the base of the internode. Method 1 is the *in situ* approach, while method 2 is the photographic approach

Appendix 3.4: Summary of regression formulae for the relationship between bark thickness (mm) and the logarithm of stem diameter (cm).

spp	Model	Unstandardized Coefficients		Standardized Coefficients	T	P	R^2	n
		B	Std. Error	Beta				
TS	(Constant)	0.270	0.142		1.895	0.079	0.625	16
	ln (stemD)	0.229	0.047	0.790	4.829	0.000		
CA	(Constant)	0.014	0.228		0.063	0.951	0.559	15
	ln (stemD)	0.372	0.092	0.748	4.058	0.001		
SB	(Constant)	-0.219	0.277		-0.792	0.440	0.701	18
	ln (stemD)	0.542	0.088	0.838	6.132	0.000		
DC	(Constant)	0.831	0.235		3.535	0.003	0.047	19
	ln (stemD)	-0.102	0.112	-0.217	-0.917	0.372		
LS	(Constant)	-0.070	0.850		-0.082	0.936	0.264	10
	ln (stemD)	0.410	0.242	0.514	1.695	0.129		
CM	(Constant)	0.441	0.518		0.852	0.413	0.022	13
	ln (stemD)	0.089	0.179	0.148	0.495	0.630		
CI	(Constant)	-0.464	0.434		-1.068	0.321	0.477	9
	ln (stemD)	0.335	0.132	0.691	2.527	0.039		

The equation is in the form $B_t = \beta_{0+} \beta_1 D$ (where B_t is bark thickness, β_0 and β_1 are regression coefficients, and D stem diameter.

Appendix 4.1: Comparisons of the log-regression coefficients of the new allometry (Researcher's) and the standard form of the empirical allometry.

spp	Colgan *et al*. (2013)		Nickless *et al*. (2011)		Shackleton (1998)		Tietema (1993)		Researcher's		Researcher's spp neutral		Colgan *et al*. (2013) spp neutral	
	β_0	β_1	β_0	β_1	β_0	β_1	β_0	β_1	β_0	β_1	β_0	β_1	β_0	β_1
TS	0.179	1.008	-0.286	1.010	-0.223	1.058	-0.495	0.968	0.103	0.912	0.042	0.962	-0.225	0.929
CA	-0.079	0.940	-0.468	1.088	---	---	-0.256	0.854	-0.318	1.017				
SB	-0.265	1.043	0.268	1.018	---	---	---	---	0.127	0.909				
DC	---	---	0.128	1.293	-0.359	1.061	-0.095	0.857	-0.210	0.980				
LS	0.167	1.018	---	---	---	---	---	---	0.132	0.925				
CM	0.239	0.895	0.295	0.911	---	---	-0.473	0.976	0.275	0.880				
CI	-0.797	1.065	---	---	---	---	---	---	0.786	1.038				
PA	---	---	---	---	---	---	---	---						

The log-regression co-efficients for the empirical allometries were derived after converting the equations from their original form $\ln(M) = \beta_0^* + \beta_1^* \ln(D^2H)$ for [Colgan *et al*. (2013), Shackleton (1998) and Tietema (1993)] and $\ln(M) = \beta_0^* + \beta_1^* \ln(D)$ for Nickless *et al*. (2011) to the standard form $\ln(M) = \beta_0^* + \beta_1^* \ln(F\rho D^2H)$. (--) shows that there is no empirical allometry for that species by that author.

Appendix 4.2: Comparisons of the factor (b) and power (a) of the new allometry equation (Researcher's) and the existing empirical allometry.

spp	Colgan *et al*. (2013)		Nickless *et al*. (2011)		Shackleton (1998)		Tietema (1993)		Researcher's		Researcher's spp neutral		Colgan *et al*. (2013) spp neutral	
	b	a	b	a	b	a	b	a	b	a	b	a	b	a
TS	0.0607	2,5323	0.027	2.7875	0.0325	2.6846	0.0326	2.455	0.0729	2.2987	0.0656	2.4172	0.0802	2.3343
CA	0.0873	2.3961	0.0383	2.7976	---	---	0.0861	2.1983	0.0536	2.6148	0.0689	2.4518	0.0959	2.3677
SB	0.02	2.6657	0.034	2.6221	---	---	---	---	0.0464	2.3281	0.0539	2.4576	0.0468	2.3733
DC	---	---	0.0457	3.1213	0.05	2.56	0.1082	2.0682	0.0733	2.3496	0.0927	2.2832	0.0959	2.2049
LS	0.047	2.4708	---	---	---	---	---	---	0.0589	2.2545	0.0809	2.3342	0.0623	2.2541
CM	0.0713	2.4007	0.062	2.4933	---	---	0.0231	2.6716	0.0699	2.3965	0.046	2.5789	0.0699	2.4904
CI	0.0237	2.8787	---	---	---	---	---	---	0.2934	2.1523	0.0411	2.6009	0.0743	2.5117
PA	---	---	---	---	---	---	---	---	0.0108	2.4361	0.0176	2.6009	0.0099	2.5117

Equations are of the form $M=bD^a$. (--) shows that there is no empirical allometry for that species by that author.

Appendix 5: The 95% confidence intervals for the slope (β_1) and intercept (β_0) used to compare the new allometry (Researcher) to the existing empirical allometries.

spp	author	β_0	SE for β_0	CI	Upper Limit	Lower Limit	β_1	SE for β_1	CI	Upper Limit	Lower Limit
TS	Colgan *et al*. (2013)	0.179	0.006	0.179±0.013	0.192	0.166	1.008	0.001	1.008±0.002	1.010	1.006
	Nickless *et al*. (2011)	-0.286	0.135	-0.286±0.289	0.004	-0.575	1.099	0.029	1.099±0.062	1.161	1.038
	Shackleton (1998)	-0.223	0.130	-0.223±0.279	0.056	-0.502	1.058	0.028	1.058±0.060	1.118	0.998
	Tietema (1993)	-0.495	0.119	-0.495±0.255	-0.24	-0.750	0.968	0.025	0.968±0.053	1.021	0.914
	Researcher	0.103	0.125	0.103±0.268	0.371	-0.165	0.912	0.027	0.912±0.058	0.970	0.854
CA	Colgan *et al*. (2013)	-0.079	0.008	-0.079±0.017	-0.061	-0.096	0.940	0.002	0.940±0.004	0.944	0.936
	Nickless *et al*. (2013)	-0.468	0.119	-0.468±0.257	-0.211	-0.725	1.087	0.031	1.087±0.067	1.153	1.02
	Tietema (1993)	-0.257	0.093	-0.257±0.200	-0.056	-0.458	0.854	0.024	0.854±0.052	0.906	0.802
	Researcher	-0.318	0.162	-0.318±0.350	0.032	-0.668	1.017	0.042	1.017±0.091	1.107	0.926
SB	Colgan *et al*. (2013)	-0.265	0.005	-0.265±0.010	-0.254	-0.276	1.044	0.001	1.044±0.002	1.046	1.042
	Nickless *et al*. (2011)	0.268	0.106	0.268±0.225	0.493	0.043	1.018	0.023	1.018±0.049	1.067	0.969
	Researcher	0.127	0.113	0.127±0.239	0.366	-0.112	0.909	0.025	0.909±0.053	0.962	0.856
DC	Nickless *et al*. (2011)	0.128	0.112	0.128±0.236	0.364	-0.108	1.293	0.041	1.293±0.086	1.379	1.206
	Shackleton (1998)	-0.359	0.092	-0.359±0.194	-0.165	-0.553	1.061	0.034	1.061±0.071	1.132	0.989
	Tietema 1993	-0.095	0.074	-0.095±0.156	0.061	-0.251	0.857	0.027	0.857±0.057	0.914	0.800
	Researcher	-0.210	0.104	-0.210±0.219	0.009	-0.429	0.980	0.038	0.980±0.080	1.06	0.900

Appendix 5: continued

spp	Author	β_0	SE for β_0	CI	Upper Limit	Lower Limit	β_1	SE for β_1	CI	Upper Limit	Lower Limit
LS	Colgan *et al*. (2013)	0.167	0.005	0.167±0.011	0.178	0.155	1.018	0.001	1.018±0.002	1.020	1.015
	Researcher	0.132	0.148	0.132±0.341	0.473	-0.209	0.925	0.027	0.925±0.062	0.987	0.863
CM	Colgan *et al*. (2013)	0.239	0.007	0.239±0.015	0.254	0.223	0.895	0.002	0.002±0.004	0.900	0.890
	Nickless *et al*. (2011)	0.295	0.184	0.295±0.405	0.700	-0.110	0.911	0.040	0.040±0.088	0.999	0.822
	Tietema (1993)	-0.473	0.197	-0.473±0.433	-0.039	-0.907	0.976	0.043	0.043±0.094	1.070	0.881
	Researcher	0.275	0.231	0.275±0.508	0.783	-0.233	0.880	0.050	0.050±0.110	0.990	0.770
CI	Colgan *et al*. (2013)	-0.797	0.007	-0.797±0.016	-0.78	-0.813	1.065	0.001	1.065±0.002	1.067	1.062
	Researcher	1.038	0.274	1.038±0.648	1.686	0.390	0.786	0.045	0.786±0.106	0.892	0.670

The equations are of the form $\ln(M) = \beta_0^* + \beta_1^* \ln(F\rho D^2 H)$.